

# Progress in the understanding of light- and elevated temperature-induced degradation in silicon solar cells: A review

Daniel Chen  | Michelle Vaqueiro Contreras  | Alison Ciesla   
 Phillip Hamer  | Brett Hallam  | Malcolm Abbott | Catherine Chan 

School of Photovoltaic and Renewable Energy Engineering, University of New South Wales, Kensington, New South Wales, 2052, Australia

## Correspondence

Catherine Chan, School of Photovoltaic and Renewable Energy Engineering, University of New South Wales, Kensington, NSW 2052, Australia.  
 Email: catherine.chan@unsw.edu.au

## Funding information

Australian Centre for Advanced Photovoltaics, Grant/Award Numbers: 1-SRI00, RG200768-B, RG200768-C; Australian Government Research Training Program, Grant/Award Number: RSAP1000; Australian Renewable Energy Agency, Grant/Award Numbers: 1-A060, 2017/RND010, 2017/RND005; Australian Research Council, Grant/Award Number: DE170100620; Institution of Engineering and Technology, Grant/Award Number: AF Harvey Engineering Prize

## Abstract

At present, the commercially dominant and rapidly expanding PV-device technology is based on the passivated emitter and rear cell (PERC) design developed at UNSW. However, this technology has been found to suffer from a carrier-induced degradation commonly referred to as 'light- and elevated temperature-induced degradation' (LeTID) and can result in up to 16% relative performance losses. LeTID was recently shown to occur in almost every type of silicon wafer, independent of the doping material. Even though the degradation mechanism is known to recover under normal operation conditions, it is a lengthy process that drastically affects the energy yield, stability and, ultimately, the leveled cost of electricity (LCOE) of installed systems. Despite the joint effort of many research groups, the root cause of the degradation is still unknown. Here, we provide an overview of the existing literature and describe key LeTID characteristics and how these have led to the development of various theories of the underlying mechanism. Further, given the continuously appearing and strong evidence of hydrogen involvement in LeTID, many mitigation methods concerning hydrogenation have been suggested. We discuss such reported methods, bearing in mind crucial consumer necessities in terms of sustained cell performance and minimised LCOE.

## KEY WORDS

degradation, hydrogen, light- and elevated temperature-induced degradation, mitigation, silicon

## 1 | INTRODUCTION

First reported in 2012,<sup>1</sup> light- and elevated temperature-induced degradation (LeTID)<sup>2</sup> was a new and unexpected degradation mechanism found to impact multicrystalline silicon (mc-Si) passivated emitter and rear cells (PERC) under typical solar cell operating conditions. With the industry set to transition production to mc-Si PERC at that time, this degradation raised significant concerns. Since then, LeTID has

been a subject of extensive research, with the root cause of the degradation still yet to be fully understood. Prior to the development of mitigation treatments, LeTID was reported to reduce the performance of devices by 10%<sub>rel</sub> typically, but up to 16%<sub>rel</sub>,<sup>3</sup> and to occur over long timescales. Surprisingly, the degradation has been recently found to also occur in higher purity materials such as Czochralski-grown (Cz-Si) and float-zoned (FZ-Si) silicon. In a similar manner to the extensively studied boron-oxygen light-induced degradation (BO-LID) in

This is an open access article under the terms of the Creative Commons Attribution License, which permits use, distribution and reproduction in any medium, provided the original work is properly cited.

© 2020 The Authors. Progress in Photovoltaics: Research and Applications published by John Wiley & Sons Ltd.

Cz-Si, the degradation is followed by a recovery in performance at conditions reachable within modules in the field when exposed to sunlight and operated in open-circuit mode ( $\sim 50^\circ\text{C}$ – $85^\circ\text{C}$ ).<sup>4,5</sup> Unlike BO-LID, however, the entire degradation and recovery process are expected to require decades under such conditions, causing a potentially huge loss in output power over a module's lifetime<sup>6</sup> and uncertainty of whether the module will even recover during this timeframe. Various treatments now exist to reduce or eliminate the impact of LeTID on silicon solar cells. This paper reviews existing literature to discuss the current understanding of LeTID and collate what is known about the defect and its key characteristics and discuss them in the context of the various explanatory theories that have been proposed.

## 2 | AN INTRODUCTION TO LETID—FIRST OBSERVATIONS

The first observation of this unique degradation behaviour was reported by Ramspeck et al.<sup>1</sup> at Schott Solar. It was not until 3 years later, in 2015, that the degradation phenomenon was coined 'LeTID' by Kersten et al.<sup>2,7</sup> to reflect the conditions under which the degradation behaviour was observed and studied, that is, under illumination at elevated temperatures. However, LeTID can also be induced via applied bias, indicating that the degradation is in fact induced by excess carrier injection thus making it more accurately described as a form of carrier-induced degradation (CID).<sup>7,8</sup> Nevertheless, the term

CID is commonly used to describe a range of other CID mechanisms in silicon including BO-LID, copper-induced light-induced degradation (Cu-LID)<sup>9,10</sup> and surface defects among others. In an attempt to distinguish LeTID from the other reported CID mechanisms, some groups later described the phenomenon as specific to mc-Si (e.g., mc-CID and mc-LID)<sup>11–15</sup> although the defect was subsequently found in various other forms of silicon. Another alternative identification that is perhaps more distinguishing, is 'hydrogen-induced degradation' (HID), as we proposed in Wenham et al.<sup>16</sup> This is due to strong indications and a consensus in recent literature that hydrogen is directly involved in the degradation process, either as a precursor for defect formation or as the LeTID defect itself. However, as the degradation under normal operating conditions will mostly occur via illumination at elevated temperatures, and there is confusion caused by the specification of the CID type, 'LeTID' has been adopted by the industry as the most standard and recognisable terminology. For the purpose of this review paper, we will be referring to the phenomenon as LeTID and the recombination active defect as the 'LeTID-related defect'.

### 2.1 | The impact of LeTID—Cells, modules and systems

Numerous reports of the impact of LeTID on a wide range of wafers, cells, modules and even some installed systems have been published. In Table 1, a list of studies on 'untreated' p-type mc-Si PERC cells and

**TABLE 1** Reported relative power and efficiency losses on p-type cells and modules without the application of LeTID mitigation strategies (refer to Section 5)

| Source             | Reference | Year | Type   | Deg. (% <sub>rel.</sub> ) | Conditions  |
|--------------------|-----------|------|--------|---------------------------|---|
| Petter et al.      | 3         | 2015 | Cell   | $\approx 16$ (η)          | $75^\circ\text{C}$ , CI (1 sun equiv.) 200 h                |
| Chan et al.        | 14        | 2017 | Cell   | 12.7 (η)                  | $70^\circ\text{C}$ , 0.46 kW/m <sup>2</sup> , 480 h         |
| Kraus et al.       | 17        | 2016 | Cell   | 11.2 (η)                  | $80^\circ\text{C}$ , 0.8 kW/m <sup>2</sup> , 325 h          |
| Luka et al.        | 18        | 2015 | Cell   | $\approx 10$ (η)          | $75^\circ\text{C}$ 1 sun, 48 h                              |
| Sen et al.         | 19        | 2020 | Cell   | 10 (η)                    | $75^\circ\text{C}$ 1 sun, 200 h (2015 cell)                 |
|                    |           |      |        | 2.5 (η)                   | $75^\circ\text{C}$ 1 sun, 200 h (2019 cell)                 |
|                    |           |      |        | 2.7 (η)                   | $75^\circ\text{C}$ 1 sun, 700 h (2019 cell)                 |
| Sen et al.         | 20        | 2020 | Cell   | 6 (η)                     | $75^\circ\text{C}$ , 1 kW/m <sup>2</sup> , 250 h            |
| Ramspeck et al.    | 1         | 2012 | Cell   | 5–6 (η)                   | $75^\circ\text{C}$ 0.4 kW/m <sup>2</sup> , 400 h            |
| Deniz et al.       | 21        | 2018 | Cell   | 4.4 (η)                   | $75^\circ\text{C}$ , CI ( $I_{SC}$ equiv.), 45 min          |
| Sio et al.         | 22        | 2018 | Cell   | 4.3 (η)                   | $65^\circ\text{C}$ , 1 sun, 5 h                             |
| Padmanabhan et al. | 23        | 2016 | Cell   | 4.3 (η)                   | $90^\circ\text{C}$ , 1 sun, 21 h                            |
| Chunlan et al.     | 24        | 2019 | Cell   | 3.2 (η)                   | $70^\circ\text{C}$ , 0.8 sun, 30 h                          |
| Fertig et al.      | 25        | 2015 | Module | 11 (P)                    | $85^\circ\text{C}$ , CI (1 kW/m <sup>2</sup> equiv.), 425 h |
| Kersten et al.     | 2         | 2015 | Module | 11 (P)                    | $85^\circ\text{C}$ , CI MPP, 400 h                          |
| Nakayashiki et al. | 26        | 2015 | Module | 10 (P)                    | Outdoors—Singapore, ~2 months                               |
| Fokuhl et al.      | 27        | 2016 | Module | 9.2 (P)                   | $85^\circ\text{C}$ , CI ( $I_{MPP}$ ), 400 min              |
|                    |           |      | Module | 7.2 (P)                   | $85^\circ\text{C}$ , CI ( $I_{SC}$ – $I_{MPP}$ ), 400 min   |
| Kersten et al.     | 6         | 2017 | Module | 7.5 (P)                   | Outdoors—Germany  |
|                    |           |      | Module | $\approx 7$ (P)           | Outdoors—Nicosia, Cyprus, 3 years                           |

Abbreviations: CI, current injection; MPP, maximum power point (current equivalent); P, power loss.

modules reported for LeTID throughout literature are compiled. The extent in apparent degradation varies significantly between different studies. Petter et al.<sup>3</sup> presented findings detailing degradation up to 16%<sub>rel</sub> on high-performance mc-Si PERC cells whereas Kersten et al.<sup>6</sup> presented field data of mc-Si PERC modules installed in both Germany and Cyprus. The modules in Cyprus were observed to have up to 7%<sub>rel</sub> power loss after 3 years of field operation and were likely to continue degrading for several years. Even in such a warm climate, the degradation alone could take a decade or more, with regeneration projected to occur on a much longer timescale. It could be inferred from the laboratory tests presented in that study that a duration of 15 years out in the field could be required before maximum degradation is reached within the specific climates, with regeneration expected to occur on a much longer time scale. As PV modules have a designated warranty of 25 to 30 years, this could pose significant issues for manufacturers, energy suppliers and consumers. Although not apparent in the table, the overall amount of reported LeTID has been reducing over time. Sen et al.<sup>19</sup> reported that cells made by one manufacturer from 2015 to 2019 has shown a >7.5%<sub>rel</sub> reduction in LeTID extent, with the majority of devices post-2018 achieving <5%<sub>rel</sub> degradation even without the employment of mitigation strategies (see Section 5), compared to 10%<sub>rel</sub> earlier. The authors note that the degree of degradation presented in Table 1 does not necessarily represent what can be optimised for in mass-production as samples are often chosen for their susceptibility to LeTID for the purpose of study.

One complication in assessing the degree of degradation and comparison between different studies, however, is the conditions used for testing. As seen in Table 1, the range of testing conditions shows large inconsistencies in the temperature, time and carrier injection technique used. We note that it has been shown that testing at elevated temperatures can result in a lower apparent extent of LeTID. This raises the need for a standard and ideally accelerated LeTID test for effective production quality checks and comparable research studies, which currently does not exist.<sup>28</sup> The International Electrotechnical Commission (IEC) has since attempted to draft and implement a standard of testing in both cells and modules, although there is still debate over the testing conditions. Currently, a proposed draft of the IEC 61215-2 ED2 (*Terrestrial photovoltaic (PV) modules—Design qualification and type approval—Part 2: Test procedures*) standard provides the specifications of LeTID testing on modules:  $75 \pm 3^\circ\text{C}$  with current injection set to a value equal to the difference between the short-circuit current of the module and the current at maximum power point (i.e.,  $I_{\text{SC}} - I_{\text{MPP}}$ ) for a duration of 162 h (+8/-0) (i.e., approximately 1 week). This is repeated until the difference in module power under STC conditions is less than 1% between two consecutive 162-h stress tests.<sup>29</sup> There is still further deliberation, however, over the conditions to be used. A testing standard proposed by TÜV Rheinland (2 PfG 2689/04.19) suggests current injection conditions of  $2 \times (I_{\text{SC}} - I_{\text{MPP}})$ , indicating that the excess carrier concentration under these conditions matches closer to those experienced by modules out in the field. This standard has been used as a placeholder for commercial module stability testing while the IEC standard is being finalised. The use of current injection

techniques for module testing is preferred over illuminated annealing as it is easier to achieve than the provision of a uniform temperature and light coverage over the entire area of a module. On the other hand, an LeTID testing standard of individual solar cells remains in the drafting stages, with IEC 63202-1 (*Measurement of light-induced degradation of crystalline silicon photovoltaic cells*) used as a guideline for testing:  $60 \pm 5^\circ\text{C}$  with steady-state illumination (irradiance of  $1000 \pm 50 \text{ W/m}^2$ ).<sup>30</sup>

A challenge for current testing procedures is that B-O-related LID can create the potential for both false positive and false negative results to occur when performing stress tests under the 2016 published version of IEC 61215, which depends on whether the B-O defects are in the dark annealed, degraded or regenerated state.<sup>31</sup> However, the errors introduced by B-O LID can be significantly reduced by the addition of stabilisation processes, consisting of a 48-h dark anneal at  $85^\circ\text{C}$  at  $I_{\text{SC}}$  conditions, before thermal cycling, humidity freeze testing or damp-heat tests. In addition, for long high-temperature tests without carrier injection (e.g., damp heat), an additional stabilisation process should be applied after the stress test. The expected errors for LeTID are reduced due to the longer timescales for reactions; therefore, a reduced impact of stress tests on the state of LeTID defects. In addition to bulk degradation, silicon nitride ( $\text{SiN}_x$ ) films and surface passivation layers are known to degrade<sup>32</sup> and even recover<sup>33</sup> after long durations of annealing under similar conditions, leading to either overestimation or underestimation of the degree of LeTID-related defect formation. In this work, however, we will focus solely on the impacts and behaviours of the bulk LeTID-related defect.

### 3 | THE KEY BEHAVIOURS OF LETID

There are several defect characteristics of LeTID that differentiate the phenomenon from other forms of CID in silicon. In this section, these key characteristics are explored.

#### 3.1 | A dependence on firing

One of the most well-known properties of LeTID is the dependence of the degradation extent on the peak temperature of the solar cell metallization or contact firing process. It was demonstrated in a number of works by Chan et al.,<sup>14</sup> Nakayashiki et al.,<sup>26</sup> Bredemeier et al.<sup>34</sup> and Eberle et al.<sup>35</sup> that LeTID is triggered by firing, with higher temperatures trending towards more severe degradation. This characteristic behaviour became a useful indicator for our later work identifying LeTID in other materials such as p-type Cz-Si wafers<sup>36</sup> and n-type silicon wafers.<sup>37</sup> Figure 1 shows the comparison between wafers fired at various temperatures between  $400^\circ\text{C}$  and  $920^\circ\text{C}$ . In several studies, LeTID was not found to occur during subsequent LeTID-stress testing if wafers were fired below approximately  $650^\circ\text{C}$  or not fired at all, but increased drastically with increasing temperatures above  $650^\circ\text{C}$ . From Figure 1A, depicting the temperature-degradation relationship for

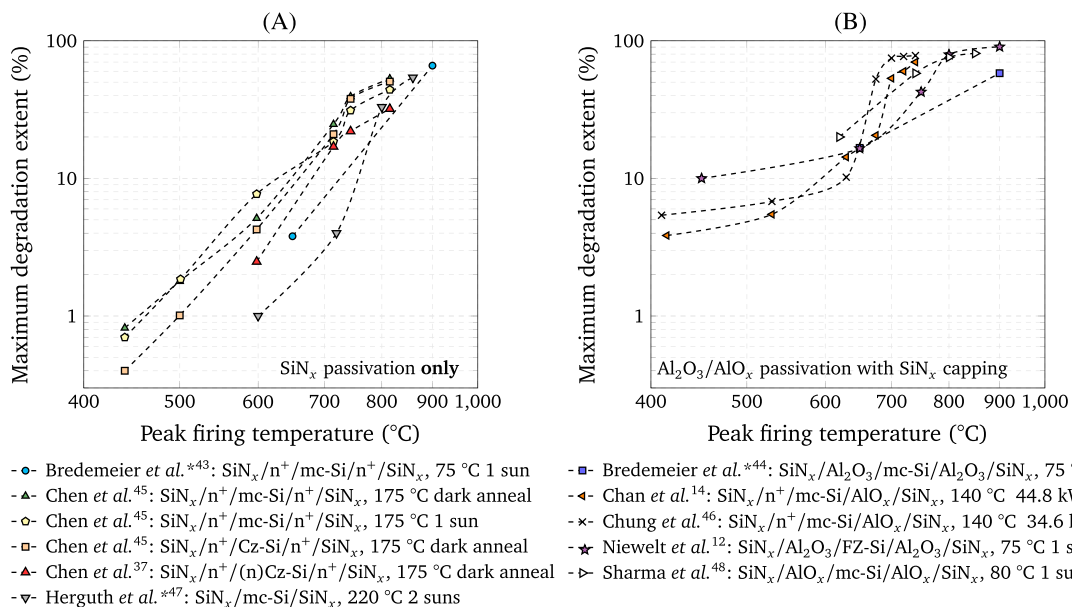


**FIGURE 1** The maximum degradation extent as a function of peak firing temperature for (A) Si<sub>N</sub><sub>x</sub> only passivated symmetrical test structures and (B) structures with at least one side AlO<sub>x</sub> or Al<sub>2</sub>O<sub>3</sub> passivated with Si<sub>N</sub><sub>x</sub> capping as extracted from previous studies.<sup>12,14,34,36–41</sup> The corresponding legends highlights the various test structures and conditions used. Lower temperatures and unfired wafers have been excluded as they typically show negligible degradation. An asterisk in the legend for the works of Herguth et al.<sup>40</sup> and Bredemeier et al.<sup>34,38</sup> indicate reported setpoint firing conditions and actual temperatures may be lower. Dashed lines are provided as a guide to the eyes

symmetrical Si<sub>N</sub><sub>x</sub> passivated test structures, an almost linear correlation with temperature is observed in several studies above 400°C on the log-log scale, indicating a possible exponential increase in the degradation extent. This relationship appears to be structure-dependent, with samples passivated with nonstoichiometric aluminium oxide (AlO<sub>x</sub>) or stoichiometric aluminium oxide (Al<sub>2</sub>O<sub>3</sub>) and capped with Si<sub>N</sub><sub>x</sub> (Figure 1B) experiencing more of an increase beyond 600°C. Although these trends are quite evident, a true comparison between the maximum degradation extent from different experiments is quite difficult as the degradation extent is affected by several factors including the material itself, testing conditions used and most importantly, the firing profile. Eberle et al.<sup>35</sup> demonstrated that a high peak firing temperature (800°C wafer temperature) with slow cooling rates can largely suppress LeTID. Thus, it appears as though both a high peak firing temperature and a relatively fast cooling rate are required for LeTID to occur.<sup>22</sup> Due to the difficulty in modifying the thermal profiles in a belt furnace, it was unclear from this study whether the cooling rate or total thermal budget was suppressing the degradation. In addition to the clear correlation between firing temperature and LeTID extent, our work also revealed an eventual decrease in the absolute effective lifetime ( $\tau_{\text{eff}}$ ) immediately after firing with conditions beyond 630°C.<sup>14</sup> The degradation of lifetime directly after firing was later attributed to pre-formed LeTID during the firing process,<sup>36</sup> the extent of which has a dependency on the quench rate during cooling. It was later found that a critical temperature of 765°C or above with a cooling rate above 50°C/s results in the formation of LeTID-related defects during firing,<sup>42</sup> conditions that are well below what is commonly experienced by PERC solar cells during contact sintering. This effect is often seen

on samples that undergo firing at high temperature followed by a degradation and recovery cycle, where the final lifetime is significantly higher than the lifetime measured after firing, with at least some portion of this increase being due to the sample already starting with a degraded lifetime after firing.<sup>43–46</sup>

### 3.2 | A universal defect in silicon

For many years, LeTID was believed to be confined to p-type mc-Si wafers and mc-Si PERC solar cells. Early evidence of degradation by Ramspeck et al.<sup>1</sup> on p-type Ga-doped mc-Si PERC solar cells was used to exclude the defect from BO-LID. Examples of unknown LID mechanisms on structures incorporating AlO<sub>x</sub> dielectric layers on the rear began surfacing with observations on Cz-Si wafers in 2015.<sup>25,47</sup> The first confirmations that LeTID also occurred on monocrystalline materials were presented in 2017<sup>36,48</sup> with more recent reports on mono-Si Ga-doped cells found in.<sup>49</sup> Fertig et al.<sup>48</sup> demonstrated that Hanwha Q-CELLS' BO-LID stabilised PERC modules would continue to experience deterioration at elevated temperatures (75°C, operated at MPP) if untreated for LeTID. At UNSW, we also carried out a systematic study on symmetrically passivated Cz-Si and mc-Si p-type test structures to compare both the degradation behaviour, as depicted in Figure 2A, and their defect recombination parameters.<sup>36</sup> For the latter, injection-dependent lifetime spectroscopy (IDLS) together with Shockley-Read-Hall (SRH) statistics was used. Comparison of the reported recombination parameters from mc-Si wafers with the obtained parameters in Cz-Si led to the conclusion of an identical

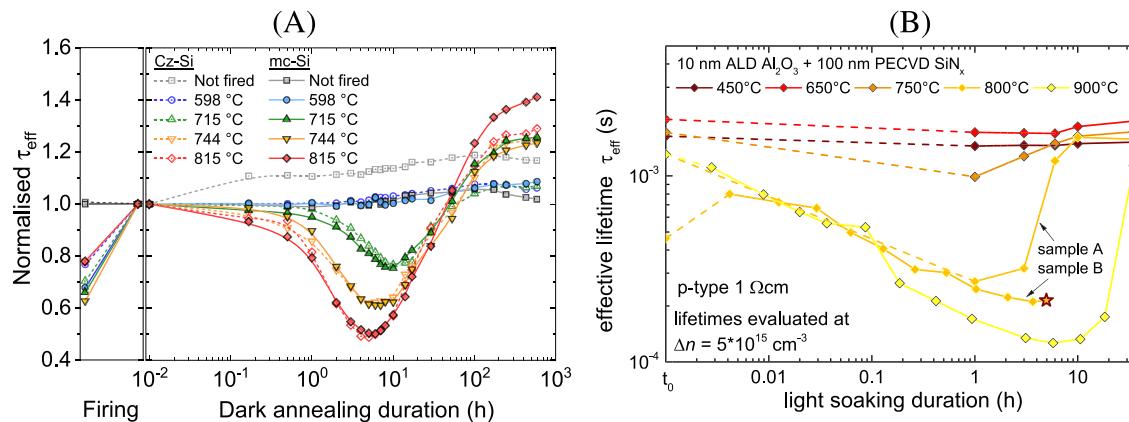


**FIGURE 2** (A) Normalised  $\tau_{\text{eff}}$  (to the value immediately after firing) as a function of dark annealing duration at 175°C of fired (from 598°C to 815°C) and not fired (NF) Cz-Si and mc-Si silicon wafers<sup>36</sup> and (B)  $\tau_{\text{eff}}$  measured on lifetime samples prepared on 1  $\Omega\text{-cm}$  p-type FZ-Si. All samples were passivated with the same dielectric layer system of 10 nm P-ALD Al<sub>2</sub>O<sub>3</sub> and 100 nm PECVD a-SiN<sub>x</sub> and only the thermal treatment after deposition was varied, as stated in the legend. The symbols denote transient QSSPC lifetime measurements evaluated at  $\Delta n = 5 \times 10^{15} \text{ cm}^{-3}$  and the connections serve as guides-to-the-eye.<sup>12</sup> (Figure 2A reprinted from Chen et al., Evidence of an identical firing-activated carrier-induced defect in monocrystalline and multicrystalline silicon, solar energy materials and solar cells, 172, 293–300, © 2017, with permission from Elsevier. Figure 2B reprinted from T. Nieuwelt, M. Selinger, N.E. Grant, W. Kwapił, J.D. Murphy, M.C. Schubert, Light-induced activation and deactivation of bulk defects in boron-doped float-zone silicon, J. Appl. Phys. 121 (2017) 185702, with the permission of AIP Publishing)

defect formation in both materials.<sup>36</sup> Since then, several previously reported degradation observations in other monocrystalline silicon wafers have been linked to LeTID. Studies on FZ-Si wafers have been shown to display novel forms of CID.<sup>12,32</sup> Such is the case of the work reported by Nieuwelt et al.<sup>12</sup> who observed a degradation on p-type FZ-Si samples passivated with Al<sub>2</sub>O<sub>3</sub>/SiN<sub>x</sub> films, fired at above 650°C (up to 900°C) and subsequently light soaked at 75 ± 5°C (Figure 2B). The recombination properties of the defects in FZ-Si are compared with mc-Si and Cz-Si in Section 4. These studies on FZ-Si facilitates opportunities to study the defect using wafers with significantly lower concentrations of metallic impurities and crystallographic defects.<sup>46</sup>

Although it is commonly held that n-type silicon wafers are less susceptible to various forms of CID,<sup>50</sup> more recent work has demonstrated the existence of LeTID in n-type materials as well.<sup>22,37,45,51</sup> Renevier et al.<sup>52</sup> investigated a form of bulk degradation in n-type Cz-Si wafers, formed on wafers coated with a SiO<sub>2</sub>/SiN<sub>x</sub> passivation scheme after rapid thermal annealing. However, this degradation was only observed when the wafers had at least one boron-diffused side. Samples either passivated in Si-rich SiN<sub>x</sub> films or Al<sub>2</sub>O<sub>3</sub> or with dual-sided phosphorus diffused layers did not show signs of degradation. The authors concluded that the degradation may originate from the interaction between the SiO<sub>2</sub> layers and the boron-doped silicon; however, no exact root cause was determined. In 2018, we later confirmed similar findings using boron- or phosphorus diffused n-type Cz-Si wafers in addition to nondiffused controls.<sup>37</sup> It was found that degradation of the n-type bulk only occurred when a diffused layer (of either polarity) was present during contact firing. The samples with a boron diffusion showed identical degradation time scales and firing dependence to LeTID in p-type, thus indicating the existence of LeTID in n-type silicon. In disagreement with Renevier et al., the phosphorus-diffused n-type wafers were also observed to degrade,

however, at a time scale several orders of magnitude faster than the boron-diffused group. This could potentially explain why previous investigations of LeTID in n-type FZ-Si wafers did not show signs of degradation, suggesting that the defect either did not form or was not recombination active in n-type or formed on a different time scale.<sup>12</sup> There has also been further studies of LeTID in n-type mc-Si wafers, in particular the work of Sio et al.<sup>22</sup> and Vargas et al.<sup>45</sup> Using direct comparisons to p-type mc-Si, both authors concluded that the degradation rate under illumination of n-type mc-Si was slower than the rates observed in p-type mc-Si under similar conditions. Although there remains a possibility that the degradation observed on different wafer types is caused by different defects, there is strong evidence and many behavioural similarities suggesting that the recombination active defect in each of these materials is the same.

### 3.3 | A dependence on dielectrics

In addition to the strong relationship between peak firing temperature and LeTID extent, several reports have repeatedly shown the crucial role of the passivation layers on the degradation. Initially, the increased degradation observed on mc-Si PERC when compared to Al-BSF devices<sup>1</sup> led to the suggestion of aluminium (Al) gettering being the underlying prevention mechanism.<sup>25,47</sup> However, the duration of time above the melting point of Al during cofiring is typically quite short (< 5 s), which would limit the gettering efficacy only to very fast-diffusing impurities or those close to the rear-surface, rendering it unlikely.<sup>53</sup> During the earlier stages, there were doubts as to whether LeTID was caused by a bulk-related defect or rather a degradation brought about by the AlO<sub>x</sub> films.<sup>25</sup> Although the dielectric layers play a significant role, numerous studies have demonstrated the

formation of a bulk defect; it has been shown by Padmanabhan et al.<sup>23</sup> and Vargas et al.<sup>54</sup> in mc-Si, and by Sperber et al. in Cz-Si<sup>55</sup> and FZ-Si<sup>56</sup> materials. Further investigations into the role played by the AlO<sub>x</sub> or Al<sub>2</sub>O<sub>3</sub> layers, which are commonly used on PERC devices, revealed degradation only occurred when samples were passivated in any combination of hydrogenated dielectric. Kersten et al.<sup>57</sup> deposited various Al<sub>2</sub>O<sub>3</sub> and SiN<sub>x</sub>:H film combinations from various tools on p-type mc-Si wafers both with and without n<sup>+</sup>-emitters present. It was observed that variations in dielectrics led to different degradation rates and confirmed that LeTID was only present on samples with dielectric layers present during firing. Soon after, Kersten et al.<sup>58</sup> also reported major differences in LeTID extent depending on the stoichiometry of the Al<sub>2</sub>O<sub>3</sub> and AlO<sub>x</sub> films by comparing dielectric deposition via atomic layer deposition (ALD), with microwave plasma-enhanced chemical vapour deposition (MW-PECVD), respectively. Their results indicate that the application of higher quality Al<sub>2</sub>O<sub>3</sub> layers led to diminished LeTID. Likewise, Vargas et al.<sup>54</sup> and Varshney et al.<sup>59</sup> showed a dependence on SiN<sub>x</sub>:H layer characteristics deposited by PECVD on the LeTID extent of mc-Si wafers, with low deposition temperatures and thinner films—both corresponding to a reduced hydrogen availability—showing the least degradation. The reasoning behind Al-BSF cells showing less LeTID than PERC cells can be explained by the fact that an Al-BSF cell contains only one hydrogen-containing dielectric layer and the full area Al contact may well be a sink for fast-diffusing hydrogen, whereas a PERC cell consists of two hydrogen-containing films, the rear of which tends to be thicker with a higher hydrogen content. The role of hydrogen will be further discussed in the context of the root cause later in Section 4.2.

### 3.4 | Spatial dependence of degradation

Another distinguishing feature of LeTID is its spatial dependence. Degradation at grain boundaries was shown to be weaker than that in

the intragrain regions of a mc-Si cell.<sup>11,60,61</sup> It was hypothesised that structural defects present at the grain boundaries inhibit LeTID defect formation<sup>11</sup> or create an internal gettering effect.<sup>60</sup> Using μ-PL imaging, Jensen et al. observed both a slower degradation and regeneration rate within a grain boundary when compared to intra-grain regions (Figure 3A). These ‘denuded zones’ of weaker degradation (Figure 3B,C), were observed by Niewelt et al.<sup>62</sup> to be approximately 200- to ~400-μm wide across a grain boundary. In the intragrain regions, degradation was shown to be homogeneous,<sup>11,62</sup> and no difference in LeTID defect density was observed between intragrain regions and dislocations.<sup>60</sup> Other studies have shown that spatial degradation properties of the observed LeTID can be extremely process dependent. A study by Lindroos et al.<sup>63</sup> found that two mc-Si sister wafers that underwent different PERC processes degraded very differently. One showed the characteristic strong homogenous degradation in the high lifetime intragrain regions and less degradation at grain boundaries, whereas the other showed weak degradation in both the intragrain regions and grain boundaries but strong degradation at the dislocation clusters. The latter was, however, attributed to nonuniform degradation of the rear surface passivation, which was stronger at the dislocations. One possible explanation would relate to the dependence of degradation on Δn, where the lower excess carrier concentrations in and around the grain boundary would result in inhomogeneities in the degradation rate.<sup>61</sup> However, it has been lately found that degradation rate variations may also arise from lateral doping differences in mc-Si wafers, which increase local currents as suggested by Mchedlidze et al.<sup>64</sup> and in agreement with the observations of Niewelt et al.<sup>62</sup> in float-zone samples. Niewelt et al. studied the degradation of p-type FZ wafers upon illumination at 75°C for several hours. They observed that wafers which had been passivated with SiN<sub>x</sub> or AlO<sub>x</sub>/SiN<sub>x</sub> stacked layers and fired at temperatures above 750°C showed the characteristic LeTID-related lifetime behaviour on a timescale of less than 30 h, as measured by QSSPC. Interestingly, from PL imaging, it was revealed that at their degraded state, the

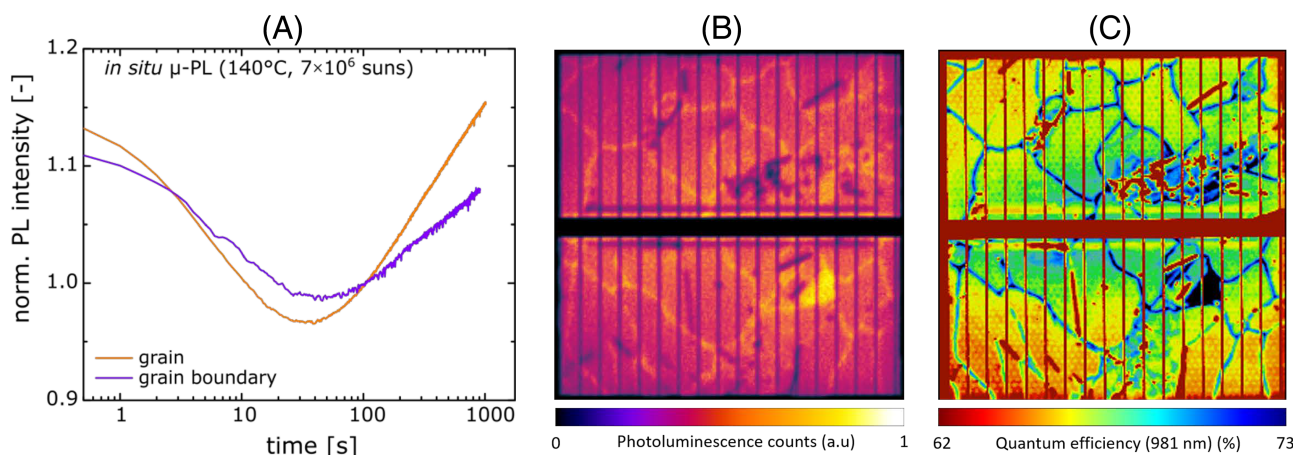


**FIGURE 3** (A) μ-PL measurements of a LeTID-sensitive sample under accelerated degradation conditions (140°C, ~7 × 10<sup>6</sup> suns) centred within a grain and a grain boundary.<sup>61</sup> (B) Photoluminescence image of a degraded (75°C, ~1 sun, 110 h) p-type mc-Si PERC solar cell highlighting denuded zones near the grain boundaries. (C) Light beam induced current (LBIC) measurement (981 nm beam wavelength) of the same cell depicting the spatial differences in quantum efficiency between grain boundaries and intra-grain regions

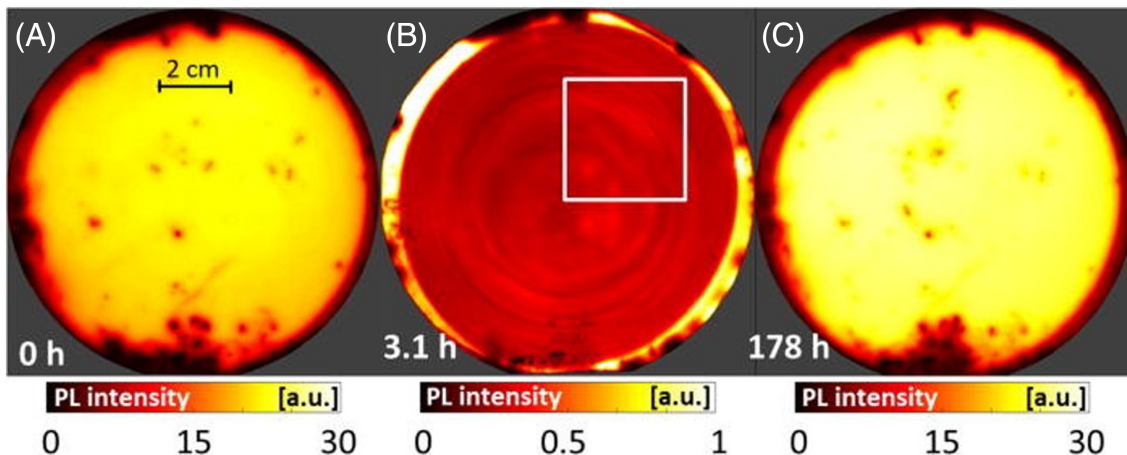


**FIGURE 4** PL images of a 1 Ω-cm p-type FZ sample passivated with 10 nm P-ALD  $\text{Al}_2\text{O}_3$ , capped by 100 nm PECVD a- $\text{SiN}_x$  and fired at 900°C. The images were taken at different stages of light induced degradation, as indicated in the image. Clear radial striations are observed in the sample after 3.1 h of light soaking.<sup>12</sup> (Reprinted from T. Nieuwelt, M. Selinger, N.E. Grant, W. Kwapił, J.D. Murphy, M.C. Schubert, light-induced activation and deactivation of bulk defects in boron-doped float-zone silicon, *J. Appl. Phys.* 121 (2017) 185702, with the permission of AIP Publishing)

samples displayed a ring pattern resembling that of the doping striations found by Lim et al.<sup>65</sup> (see Figure 4). Even though no conclusive evidence was provided on Nieuwelt's study, it was argued that the relative changes in PL intensity with degradation (up to 10%) could not be solely accounted by the doping variation in FZ wafers (<5%). Nevertheless, from Mchedlidze's recent capacitance-voltage results on mesa diodes fabricated from commercial PERC mc-Si solar cells, an almost linear correlation between doping concentration and relative degradation from electroluminescence (EL) imaging was found, as shown in Figure 5.<sup>64</sup> To our knowledge, this is the first time that such a clear correlation between doping and relative degradation has been reported in literature. Despite the fact this correlation is not

conclusive on the constituents of the LeTID defect, it suggests dopants are at least interacting to alter the LeTID kinetics and deserves further analysis.

### 3.5 | Degradation and regeneration models and kinetics

#### 3.5.1 | LeTID transition-state modelling

The rate at which the lifetime of the wafer degrades and recovers during an LeTID cycle is important in helping identify the root cause, determining the total impact of the degradation and in developing mitigation strategies. As a result, many studies have focussed on this topic. A practical way of expressing the behaviour of the defect is through a state-diagram with three states: (A) predegradation; (B) degraded and (C) recovered, with key transitions between those states. The earliest models presented by Krauß et al.<sup>17</sup> and Sperber et al.<sup>66</sup> adapted the three-state model that resembled those historically used to describe BO-LID behaviour to demonstrate similar resemblances in defect evolution.<sup>17,66</sup> The most widely used version is presented in Figure 6. The defect evolves from a recombination inactive State A into a degraded State B and eventually into a recovered and stable State C (see Figure 6). The maximum extent of LeTID is determined by the balance between the degradation rate ( $A \rightarrow B$ ,  $R_{deg}$ ) and the recovery rate ( $B \rightarrow C$ ,  $R_{reg}$ ). Noting that several works suggest a possible reversible reaction from the degraded state back into the inactive state (B to A), analogous to B-O dissociation. Although later studies also observed a two-step degradation (fast and slow forming defects),<sup>67,68</sup> a single transition between State A and State B is widely presented. This simplified model is valid when the fast-forming component is negligible or no longer observed under accelerated testing conditions.<sup>69</sup> It is, however, worth pointing out

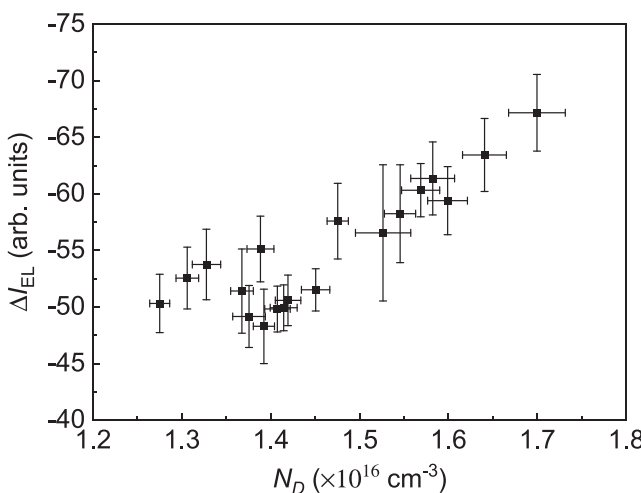


**FIGURE 5** Measured doping concentration of a set of mesa diodes fabricated from a commercial mc-Si solar cell plotted against the EL-relative degradation of the sample upon forward-current biasing at 70°C.<sup>64</sup> (© 2017 WILEY-VCH Verlag GmbH & Co. KGaA, Weinheim)

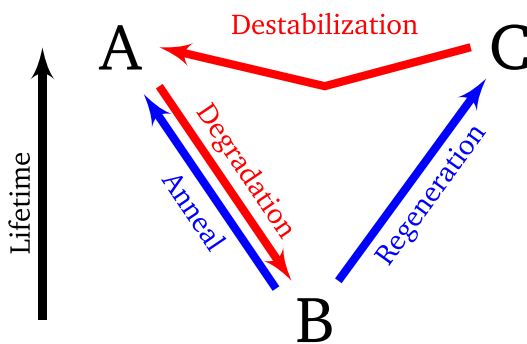


**FIGURE 6** Illustration of a three-state defect model and associated reaction pathways for charge carrier lifetime degradation and regeneration in boron-doped FZ silicon.<sup>66</sup> (© 2017 WILEY-VCH Verlag GmbH & Co. KGaA, Weinheim)

that unlike BO-LID where defect formation can occur independent of recovery under low intensity illumination, LeTID-related degradation and recovery occur simultaneously.<sup>70</sup> Further experiments carried out by Sperber et al.<sup>66</sup> demonstrated an instability of the defect in the recovered state through the application of a short dark annealing treatment for 5 min at 200°C. Subsequent illuminated annealing would see the carrier lifetime of samples re-degrade followed by another subsequent recovery. The dark annealing did not result in a change in the carrier lifetime, and for this reason, a direct transition from State C back to the inactive State A was postulated to occur without reverting through State B.

The state diagram presented in Figure 6 is able to describe many, but not all, behaviours of LeTID. An expansion to the model was proposed by our group based on the impact of dark annealing on defect destabilization.<sup>69</sup> By subjecting wafers to a cyclic process of illuminated annealing followed by dark annealing treatments, Fung et al. identified that recovery under light was not permanent. With each dark annealing step at a higher temperature of 232°C for 8 min, a subsequent illuminated anneal (conducted at 135°C, illumination intensity of 25.7 kW/m<sup>2</sup>) would initiate another degradation and recovery cycle. However, after continued cycling, an exponential reduction in the maximum LeTID-related lifetime to a non-zero steady-state is observed (Figure 7). It was thus concluded that the dark annealing process was producing additional defect precursors that remained in a state of inactivity in the dark but would later activate under

illumination. To account for this, a new recombination inactive reservoir state (State R), which would feed into State A, was introduced. To explain the reduction in maximum degradation extent after each cycle, one plausible explanation was that the reservoir volume would be present after firing, and would systematically deplete during dark annealing and where the reverse reaction from State A back into the reservoir or from State C back into State A did not occur. With each cycle, however, the maximum degradation converges towards a certain limit and the degradation could not be entirely suppressed. One interpretation for this observation would be that a defect in State B would revert back into a mobile defect precursor, which then binds with another nearby element to form the metastable yet inactive State A. If the concentration of the other element were to stay constant (e.g., dopant atoms and other slow diffusing impurities), as the concentration of the defect precursor decreases, it may become increasingly difficult for defect precursors formed in subsequent cycles to avoid rebinding back into State A.<sup>69</sup>

### 3.5.2 | Modulating the defect kinetics

The LeTID defect model tends to be more complex than similar models used to describe other forms of LID in silicon. There are multiple factors that influence the kinetics and the influence of these factors tend to convolute the results.

#### Excess carrier concentration

One of the earlier systematic studies on p-type mc-Si LeTID provided evidence of the prominent role of excess carrier concentration ( $\Delta n$ ) on LeTID kinetics.<sup>2</sup> Degradation tests revealed that the reaction kinetics were greatly impacted by the different test modes ( $V_{OC}$  or  $I_{SC}$ ) applied to modules. Operating at  $I_{SC}$ , where the excess carrier concentrations are significantly lower, led to a reduced  $R_{deg}$  whereas operating at  $V_{OC}$  demonstrated quicker degradation and recovery rates (Figure 8). Under the same operating condition, increasing the temperature leads to an increase in both  $R_{deg}$  and  $R_{rec}$ . It was also shown that better passivated samples led to faster kinetics, as reduced surface recombination facilitated larger  $\Delta n$ .

In the same work, the relative degradation extent of cells made from wafers of known brick height, tested at 60°C and 1 kW/m<sup>2</sup> for a period of 24 h, was reported. Even though this short duration test

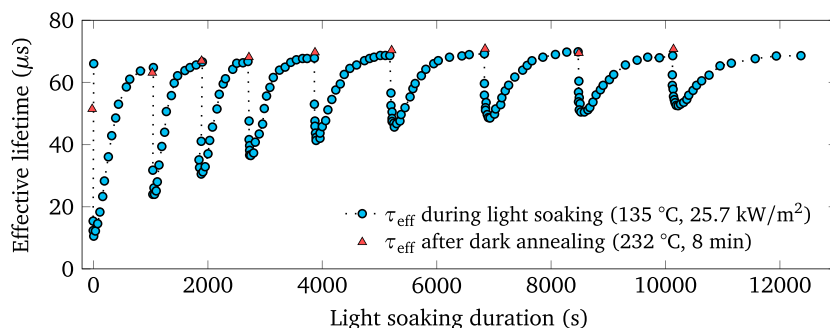


**FIGURE 7** Relative change in the effective lifetime with light soak duration for a mc-Si lifetime sample subjected to dark anneal–Light soak cycles, where the dark anneal was applied after each complete degradation and recovery cycle<sup>69</sup>

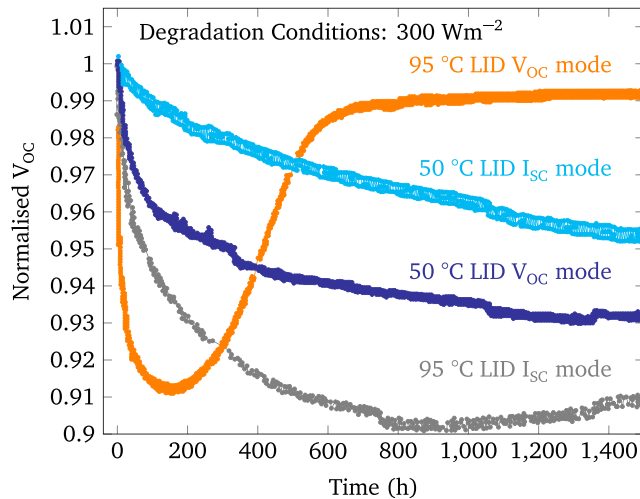


**FIGURE 8**  $V_{oc}$  data of four mc-PERC cells during illumination at two temperatures and operational modes (50°C and 95°C;  $V_{oc}$  and  $I_{sc}$  mode).<sup>2</sup> (Reprinted from Solar Energy Materials and Solar Cells, 142, F. Kersten, P. Engelhart, H.-C. Ploigt, A. Stekolnikov, T. Lindner, F. Stenzel, M. Bartzsch, A. Szpeth, K. Petter, J. Heitmann, J.W. Müller, Degradation of multicrystalline silicon solar cells and modules after illumination at elevated temperature, Sol. Energy Mater. Sol. Cells. 142 (2015) 83–86. https://doi.org/10.1016/j.solmat.2015.06.015. Degradation of multicrystalline silicon solar cells and modules after illumination at elevated temperature, 83–86, Copyright © 2015, with permission from Elsevier)

cannot reveal much about the final extent of degradation, the results suggest significantly faster degradation rates on cells made from the bottom of the brick, which agrees with the observations in,<sup>39</sup> where the degradation extent was also evaluated. Many more studies on the dependence of LeTID kinetics on illumination,<sup>14</sup> dopant type<sup>43,45,51</sup> and doping concentration,<sup>64</sup> among others, have been published. What is important to note, however, is that all these reports converge at demonstrating that the key factor readily impacting the LeTID kinetics is that of the excess carrier availability. This is independent of their generation origin, that is, photogenerated or as the result of applied current. Therefore, accurate LeTID kinetics studies become a challenging task due to the variations in structural<sup>43</sup> and point defect densities and nonuniform doping. Kwapis et al.<sup>67</sup> conducted a much more carrier-injection-controlled study of the degradation kinetics on a range of boron-doped mc-Si samples. Their findings showed an almost linear correlation between excess carrier concentration and the degradation rate, suggesting the interaction of a single carrier (electron) in the defect formation kinetics. A relationship between  $\Delta n$  and the regeneration rate, however, requires further unravelling.

#### Dark annealing and thermal history

The same LeTID-defect activated during illumination has been shown to be activated whilst annealing in the dark at 175°C.<sup>36,71</sup> However, the degradation ( $R_{deg}$ ) and regeneration rates in the dark ( $R_{reg}$ ) were significantly slower and the degradation extent much less than in the light. Similar results were reported in<sup>72</sup> although it was also shown

that DA at 75°C showed no degradation during the experiment length of 200 hours. Moderate temperature dark anneals have thus been recently applied to study the LeTID-related defect and kinetics in the dark,<sup>37</sup> with the benefits of faster testing in comparison to the illuminated tests at 75°C, and most importantly, reducing the activation of other light-induced defects such as BO-LID.

The reaction kinetics of LeTID are heavily dependent on the thermal history of the sample. Thus, dark annealing does not restore the initial state of the wafer, it rather puts it into a new state, where very different degradation and regeneration may occur. This has been shown in Chan et al.,<sup>73</sup> where a systematic study of the effect of various dark anneals prior to LeTID testing at 75°C and 1 kW/m<sup>2</sup> was reported. Such treatments will be referred to as 'pre-DA' from here on. In that work, a 2.5 h pre-DA was applied to finished p-type mc-Si solar cells using temperatures ranging from 200°C to 250°C (Figure 9). The application of the pre-DA at temperatures of 200°C or below were found to accelerate the subsequent degradation and regeneration rate and increase LeTID extent (Mode 2), whereas at higher temperatures, the subsequent degradation and regeneration rate were significantly slowed and LeTID extent was suppressed (Mode 4). Annealing in the dark can therefore act as a mitigation strategy, as will be discussed in Section 5. Further investigations tracked the LeTID defect formation during the pre-DA treatment itself at 232°C for various times up to 2.5 h, followed by LeTID tracking at 75°C and 1 kW/m<sup>2</sup>, as reported in Liu et al.<sup>44</sup> It was shown that the so-called 'stage' of the dark degradation and recovery cycle, which the sample was at when the pre-DA was stopped (i.e., before any degradation, during the degradation or during or after the regeneration), modulated the subsequent illuminated degradation kinetics to a similar extent, as previously shown in Chan et al.<sup>73</sup> The results demonstrated that there is a significant influence of even short duration pre-DA treatments on the subsequent LeTID kinetics, particularly at temperatures where the involvement of other activated defects are

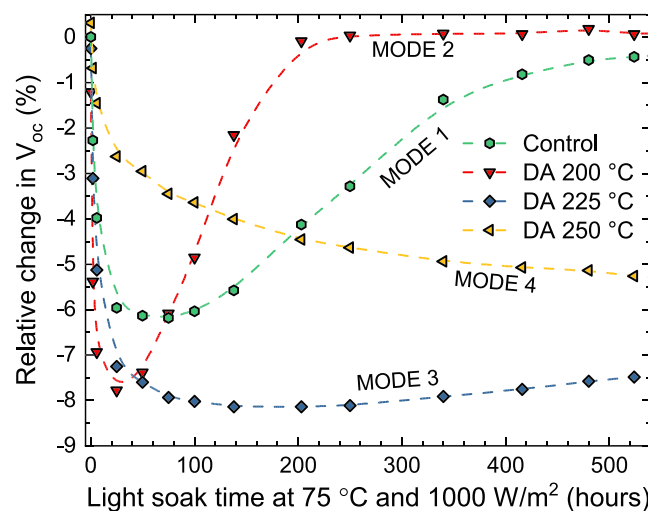


**FIGURE 9** Degradation and regeneration curves highlighting the four distinct modes of the defect evolution during light soaking as a result of pre-degradation dark annealing at different temperature<sup>73</sup>

more likely to occur.<sup>43,73</sup> This, in turn, further complicates the ability to predict and compare LeTID behaviour across multiple studies.

## 4 | EVALUATION OF THE ROOT CAUSE

There have been numerous studies attempting to uncover the defect responsible for LeTID, however, identifying a specific defect in silicon out of thousands can sometimes be tricky. Nevertheless, the list of suspects can be greatly narrowed down through a range of characterisation techniques. One of these extensively used techniques is lifetime spectroscopy, namely, IDLS and the more advanced, temperature- and injection-dependent lifetime spectroscopy (TIDLS).<sup>74</sup> With these techniques, a fit of the SRH-related lifetime, isolated from the effects of intrinsic- and surface-related lifetime components, can then yield the capture-cross-section ratio ( $k$ -value) pertaining to a specific defect. This  $k$ -value is defined by a ratio between the electron and hole capture cross-sections ( $\sigma_n$  and  $\sigma_p$ , respectively) given by<sup>75</sup>

$$k = \frac{\sigma_n}{\sigma_p} = \frac{\tau_{p0}}{\tau_{n0}} \times \frac{v_{th,h}}{v_{th,e}},$$

where  $v_{th,h}$  and  $v_{th,e}$  are the thermal velocities of holes and electrons, respectively,  $\tau_{n0}$  and  $\tau_{p0}$  are the electron and hole capture time

constants, respectively. In Table 2, a collection of reported defect  $k$ -values and apparent defect energy levels (both extracted and assumed) for diverse LeTID-affected materials are collated. These characteristic values have served as a starting point for the various efforts on the identification of the LeTID responsible defect which will be discussed in this section. Here, we consider the evidence for and against each of the suggested responsible defect candidates, with a focus on the possible role of metals and hydrogen on the degradation.

### 4.1 | Are metals to blame?

Metallic impurities were one of the earliest proposed causes for LeTID. To explain experimental observations, Bredemeier et al.<sup>34</sup> proposed a model consisting of latent metallic precipitates ( $M_p$ ) grown into the ingot as depicted in Figure 10. During firing at high temperatures ( $>650^\circ\text{C}$ ), these metal precipitates dissolve into mobile, likely interstitial, metal atoms ( $M_i$ ), whereas at lower firing temperatures, these precipitates are assumed to not (or only partly) dissolve. Due to the rapid quenching, these  $M_i$  atoms are thought to then bond weakly with a homogeneously distributed impurity to form a recombination inactive  $M_i-X$  complex, for which H has been recently proposed as a likely candidate by the same authors.<sup>82</sup> During illuminated annealing, this complex is conjectured to alter configuration into a slightly more recombination active complex,  $M_i - X^*$ , to explain observations of an

**TABLE 2** List of literature-reported capture cross-section ratios and apparent defect energy levels measured for LeTID on various silicon materials

| Source             | Reference     | Type      | Method | $k$ Value  | Energy Level  |
|--------------------|---------------|-----------|--------|--|---|
| Bredemeier et al.  | <sup>38</sup> | (p) mc-Si | IDLS   | $20 \pm 7$   | None stated   |
| Nakayashiki et al. | <sup>26</sup> | (p) mc-Si | IDLS   | 28.5   | $-0.26 \text{ eV} < E_t - E_i < 0.24 \text{ eV}$  |
| Morishige et al.   | <sup>76</sup> | (p) mc-Si | IDLS   | $26 < k < 36$  | $-0.27 \text{ eV} < E_t - E_i < 0.13 \text{ eV}$  |
| Vargas et al.      | <sup>13</sup> | (p) mc-Si | TIDLS  | Upper bandgap: $49 \pm 21$<br>Lower bandgap: $56 \pm 23$       | Upper bandgap: $E_t - E_i = 0.21 \pm 0.05 \text{ eV}$<br>Lower bandgap: $E_t - E_i = -0.32 \pm 0.05 \text{ eV}$ |
| Jensen et al.      | <sup>77</sup> | (p) mc-Si | TIDLS  | Upper bandgap: $23.5 \pm 5.6$<br>Lower bandgap: $23.9 \pm 5.5$ | Upper bandgap: $E_t - E_i = 0.1 \pm 0.07 \text{ eV}$<br>Lower bandgap: $E_t - E_i = -0.21 \pm 0.06 \text{ eV}$  |
| Chen et al.        | <sup>36</sup> | (p) mc-Si | IDLS   | $33.4 \pm 1.5$   | Assumed mid-gap   |
| Fung et al.        | <sup>69</sup> | (p) mc-Si | IDLS   | $27 < k < 35$  | None stated   |
| Sen et al.         | <sup>78</sup> | (p) mc-Si | IDLS   | $29 \pm 4$   | Assumed mid-gap   |
| Winter et al.      | <sup>79</sup> | (p) mc-Si | IDLS   | $29a \pm 1$  | None stated   |
| Chen et al.        | <sup>36</sup> | (p) Cz-Si | IDLS   | $39.4 \pm 4.9$   | Assumed mid-gap   |
| Kim et al.         | <sup>80</sup> | (p) Cz-Si | IDLS   | $36 \pm 2$   | None stated   |
| Chen et al.        | <sup>37</sup> | (n) Cz-Si | IDLS   | $0.028 \pm 0.003$  | Assumed mid-gap   |
| Kang et al.        | <sup>81</sup> | (p) ML-Si | IDLS   | $20 \pm 7$   | Assumed mid-gap   |
| Niewelt et al.     | <sup>62</sup> | (p) FZ-Si | IDLS   | 35   | Assumed mid-gap   |
| Sperber et al.     | <sup>66</sup> | (p) FZ-Si | IDLS   | $20 \pm 2$   | None stated   |
| Niewelt et al.     | <sup>12</sup> | (p) FZ-Si | IDLS   | $30 (35^a) \pm 10$   | None stated   |
| Kang et al.        | <sup>81</sup> | (p) FZ-Si | IDLS   | $20 \pm 7$   | Assumed mid-gap   |

Abbreviation: ML-Si, mono-like silicon.

<sup>a</sup>Q-factor.

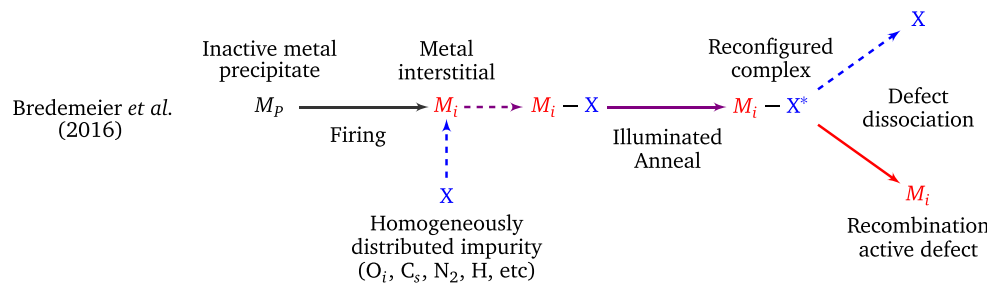


**FIGURE 10** A simplified model for the involvement of metal impurities as adapted from the theory proposed by Bredemeier et al.<sup>34</sup> This graphic representation is for illustrative purposes only

initially fast-forming recombination centre seen in Bredemeier et al.<sup>38</sup> With continued illuminated annealing, the  $M_i - X^*$  complex dissociates into its constituents, releasing the recombination active  $M_i$ , which subsequently causes the degradation. The regeneration mechanism would then be related to the diffusion of the mobile interstitials over time to the wafer surface or any crystallographic defects which may act as sinks.

In a following experiment, by using wafers of different thickness, Bredemeier et al.<sup>83</sup> concluded that LeTID regeneration could be explained by the diffusion of a recombination active species towards the wafer surfaces. The expected diffusion coefficient at 75°C was in the range of  $D = (5 \pm 2) \times 10^{-11} \text{ cm}^2/\text{s}$ , matching closely with those of Ni and Co species. However, the diffusion coefficient also matched closely to that of hydrogen, thus, it was also proposed that hydrogen in-diffusion from the surface could lead to a passivation of the defect and hence, recovery. Jensen et al.<sup>84</sup> also observed Ni-rich precipitates that were later also observed in a study by Deniz et al.<sup>21</sup> to be decorating dislocations or stacking faults. However, these observations cannot explain the largely homogeneous nature of degradation seen across mc-Si grains<sup>62</sup> as discussed in Section 3.4. Furthermore, on mc-Si wafers, denuded (or defect-free) zones of approximately 100  $\mu\text{m}$  were observed around grain boundaries,<sup>11,62,85</sup> which would rule out any slow diffusing elements (including  $\text{Mo}_i^{0/+}, \text{W}_i^{0/+}, \text{Ti}_i^{+/++}$ ) as they simply cannot move far enough under any high-temperature step of the solar cell manufacturing process.<sup>84</sup> Wagner et al.<sup>86</sup> correlated the amplitude of LeTID degradation with various detected impurities across the length of a Cz-grown ingot including interstitial oxygen ( $O_i$ ), substitutional carbon ( $C_s$ ), iron (Fe), chromium (Cr), Cu, aluminium (Al), Ni and Ti. A linear correlation between the distributed concentration of Al and the extent of LeTID was presented, in addition to a quadratic dependency on the  $O_i$  concentration above a specific critical value ( $O_i \sim 1 \times 10^{18}/\text{cm}^3$ ). It was also noted that no alterations were applied to the  $\text{SiN}_x:\text{H}$  films and using the assumption that the hydrogen content would be comparable between samples, the authors were not able to draw any conclusions regarding the involvement of hydrogen. With a wide range of impurities in the ingot studied, correlation does not necessarily equate to causation; however, the involvement of oxygen appears to be important, and further confirmation is still required.

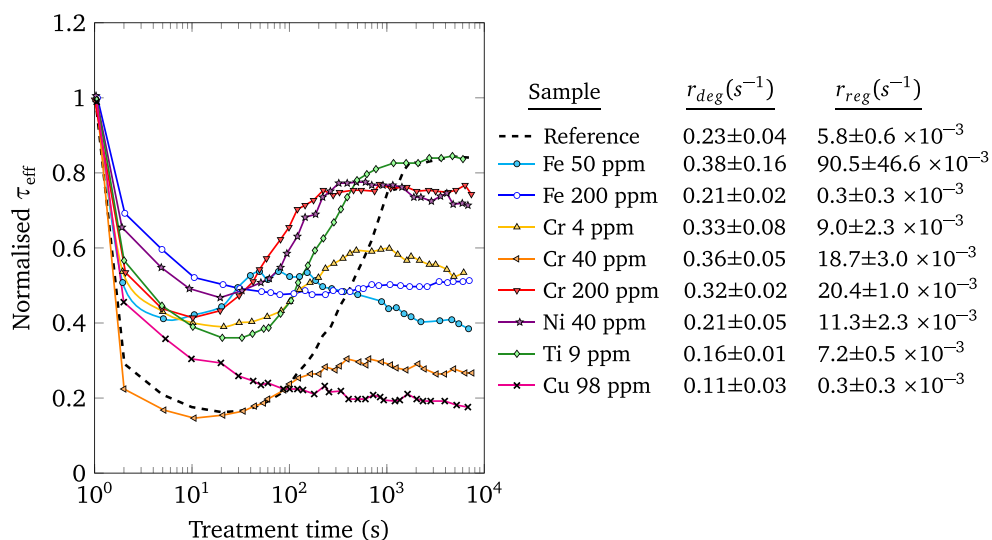
Studies on fast-diffusing metallic impurities in samples with LeTID have been reported using a range of techniques. Luka et al.<sup>84</sup> and Jensen et al.<sup>87</sup> both reported Cu precipitates located within the grain boundaries of LeTID susceptible wafers using elemental micro-

analysis techniques such as energy-dispersive X-ray spectroscopy (EDX) and micro-X-ray fluorescence ( $\mu$ -XRF), respectively.<sup>84,87</sup> Ylikoski et al. further applied a Cu precipitation model to explain the impact of a dark annealing process conducted prior to light soaking for LeTID formation. The study found that higher temperature (300°C) annealing for several hours suppressed the formation of LeTID, whereas for a shorter duration (0.5 h) or at lower temperature (<250°C), the heat treatments led to a much stronger LeTID. This is consistent with a possible defect mechanism associated with metal precipitation and dissolution.<sup>88</sup> Interestingly, the confirmation of LeTID in n-type silicon may consequently rule out the role of Cu in LeTID as discussed in Chen et al.<sup>37</sup> Although Cu-LID has been observed in n-type silicon, it is typically only seen in very lightly doped wafers, for example, in the excess of 5  $\text{k}\Omega\cdot\text{cm}$  as in Savin et al.<sup>89</sup> In n-type silicon, a lower concentration is required to initiate the nucleation of precipitates since the Fermi-level of the material is closer to the electron neutrality level of precipitates (approximately at  $E_C - 0.2 \text{ eV}$ ).<sup>90</sup> Thus, the effects of Cu contamination on the carrier lifetime in n-type are not only observed to be more severe than for p-type with identical concentrations, but the effects of precipitation would also occur immediately after Cu in-diffusion and without the need for carrier injection.<sup>90,91</sup>

Understandably, the binding energies of various impurities with hydrogen may differ strongly, leading to very different LeTID behaviour depending on the dominant binding partner. One of the studies in<sup>92</sup> intentionally contaminated p-type mc-Si wafers with quantities of Fe, Cr, Ti, Ni and Cu in an effort to understand the impact of these impurity concentrations on the rate of LeTID degradation and recovery (Figure 11). Although the results showed a wide range of degradation and recovery rates, it was not possible to distinguish the effects of different hydrogen complex binding energies from other light-induced defects (Fe, Cu), the impact of different resistivities and inherently variable  $\tau_{\text{eff}}$  (leading to varying  $\Delta n$ ) based purely on lifetime spectroscopy analysis.

One last notable behaviour supporting the hypothesis of a metal-induced defect is the effect of impurity gettering procedures on the severity of LeTID as first noted by Zuschlag et al.<sup>93</sup> and later in various other studies.<sup>94,95</sup> Zuschlag et al. observed that by applying phosphorus diffusion gettering (PDG) processes and emitter removal, the subsequently passivated and fired wafers exhibit a reduction in LeTID implying the possible removal of an involved defect constituent or precursor. We note that a study by Chakraborty et al.<sup>95</sup> also claimed to observe LeTID reduction through gettering on wafers and cells;

**FIGURE 11** Evolution in normalised  $\tau_{\text{eff}}$  of mc-Si samples contaminated with various concentrations of metal impurities (Fe, Cr, Ni, Ti, Cu) as a function of laser-treatment ( $45 \text{ kW/m}^2$ ,  $140^\circ\text{C}$ ) duration. Legend contains corresponding extracted degradation and regeneration rates. This figure is adapted using data from Vargas<sup>92</sup>



however, the lifetime test structures in that study were not fired, a prerequisite for observing LeTID. When a phosphorus diffusion is used to both form an emitter and perform gettering on solar cells, the differences in the front surface emitter profiles of the cell with and without gettering prevent a conclusive link between LeTID extent and the gettering process being drawn. There has been some degree of contradiction to these findings in the work of Sperber et al.<sup>96</sup> and our own.<sup>37</sup> In the former, the application of a  $\text{POCl}_3$  diffusion process at  $840^\circ\text{C}$  for  $\sim 45$  min to p-type FZ-Si wafers led to the observation of very similar degradation behaviour independent of the gettering process, suggesting that the defects responsible for LeTID in FZ-Si are not significantly affected by the PDG process.<sup>96</sup> Whereas, our observations in Chen et al.<sup>37</sup> on n-type Cz-Si wafers showed that LeTID would only manifest in fired samples with diffused layers. We concluded in that work that the emitter was required as a catalyst during firing to introduce a precursor of LeTID into the wafer; however, degradation occurred irrespective of whether or not the emitter was present post-firing.<sup>37</sup> The heightened degradation following a high-temperature diffusion would be in contradiction with the theory that gettering could help to suppress the degradation. It is worth mentioning that virtually all PERC solar cells are effectively put through a PDG process during solar cell fabrication.

The occurrence of LeTID in FZ-Si wafers, however, puts into question the likelihood of metallic impurities as a cause for LeTID. Instead, it leaves several nonmetal impurities as likely candidates. Niewelt et al.<sup>46</sup> and our discussion in Chen et al.<sup>37</sup> both argued that intrinsic defects such as silicon self-interstitials and lattice vacancies may have an involvement in LeTID. The latter was later tested in a study by Khan et al.,<sup>97</sup> where vacancy formation was induced via electron irradiation. It was found that vacancy-related defects had vastly different SRH characteristics ( $k$ -value between 1.6 and 7.5) to that of LeTID and that contact firing would instead eliminate any radiation-induced defects. The current research in identifying any link between non-metal impurities and LeTID remains largely unexplored, and thus concrete conclusions are yet to be drawn. If we quickly relate to the

notion of a hydrogen activated defect (Section 4.2), it is well established that the availability of monatomic hydrogen has dependencies on the concentration of sinks for hydrogen and in the case for silicon, this is commonly in the form of crystallographic or point defect impurities (e.g., dopant atoms). It may be the case that almost all impurities including vacancies, oxygen, carbon or other metals—which are all well known to pair with hydrogen—will act as a sink for atomic hydrogen, which, upon thermal or light-activated dissociation, would then show a positive correlation with the LeTID defect concentration. If not directly observed by electrical or optical means it may be only possible to identify the involved impurities by thorough studies on intentionally contaminated, high-resistivity and high carrier lifetime silicon crystals.

## 4.2 | Hydrogen: A likely candidate

The overall dependence on the firing conditions (Section 3.1) and the need for a hydrogen containing dielectric to be present during firing (Section 3.3) led to the first hypotheses: the possible involvement of hydrogen diffusing in from the surface dielectric films<sup>85</sup> in defect activation or as a part of the defect itself. There have been, however, a mixed range of ideas regarding the exact role of hydrogen in LeTID. Nakayashiki et al.<sup>26</sup> proposed a theory as to how hydrogen may reduce the recombination activity of the defect. Under illumination, the change in charge state of a hydrogen passivated defect causes the hydrogen to dissociate, thus returning the defect to its recombination active state. In the dark, the return of the quasi-Fermi levels back towards the valence bands returns the constituent atoms back to their original charge state and the hydrogen repassivates the defect. Although this theory does not account for the observations of defect formation and regeneration under identical conditions in the dark, it is nonetheless, similar to the proposal of Bredemeier et al. discussed earlier that hydrogen initially passivates a metallic impurity after firing. The case of hydrogen being responsible for both degradation and

regeneration was also considered in Chan et al.,<sup>73</sup> whereby one hydrogen atom could activate a defect, whereas a second atom could subsequently passivate the defect.

#### 4.2.1 | A direct correlation with hydrogen

Most studies investigating the influence of hydrogen on LeTID have done so in two primary ways: by either (1) manipulating the hydrogen content within the passivating dielectric films or (2) indirectly correlating the influence of firing profiles and thermal treatments on hydrogen diffusion. Recently, studies have demonstrated a more direct involvement of hydrogen in instigating LeTID-related degradation.<sup>56,82,98</sup> A study by Jensen et al.<sup>98</sup> used microwave-induced remote hydrogen plasma (MIRHP) on p-type mc-Si wafers as a method of introducing hydrogen, which led to the formation of an LeTID-like defect. Samples heated to identical temperatures and durations in the absence of a hydrogen plasma, however, did not degrade. Jensen et al.<sup>98</sup> concluded that the presence of a hydrogen source was essential for degradation, however, the time-temperature firing profile was not a necessity. This confirms that on samples with an alternative source of hydrogen, such as a hydrogenated dielectric layer, the firing process would only provide a means of introducing the hydrogen into the bulk, rather than directly activating LeTID. A similar form of LeTID may have also been activated using a shielded hydrogen plasma process on p-type FZ-Si wafers in a study by Bourret-Sicotte et al.<sup>99</sup> These results would further explain LeTID-related degradation occurring in pre-hydrogenated wafers where the dielectric layers were subsequently removed after firing.<sup>100</sup>

Interestingly, a unique example of LeTID formation in the absence of firing is presented in the work of Sperber et al.<sup>56</sup> In this example, unfired and undiffused boron-doped p-type FZ-Si wafers exhibited LeTID-related degradation directly after the direct-PECVD deposition of dielectric layers, almost to the same extent as wafers fired at high temperature (850°C). It was postulated that the 400°C PECVD deposition step may possibly allow enough hydrogen into the silicon bulk to cause LeTID, even though commonly applied PECVD deposition processes for passivating layers use similar temperatures without LeTID activation in the absence of a firing step. One possible explanation could be the difference in deposition tools, that is, direct-PECVD compared to remote-PECVD, for which the former is known to be able to lead to more H-rich films.<sup>101</sup> The direct exposure of silicon to hydrogen containing plasma in a direct-PECVD reactor is also well known for introducing hydrogen into the silicon bulk, usually for defect passivation.<sup>102</sup> A simpler explanation may be the absence of hydrogen sinks associated with higher quality FZ-Si wafers. Besides boron, the reduced number of sites where hydrogen may be trapped allows for a deeper penetration into the bulk even at low temperatures, whereas in Cz-Si and mc-Si, the high impurity concentrations confine hydrogen to within a few microns of the surface.

The direct quantification of low concentrations of hydrogen in silicon is often quite difficult. This is often due to the detection limitations of characterisation tools, the high mobility of hydrogen species

even at room temperature,<sup>103</sup> the impact of characterisation techniques on hydrogen<sup>104,105</sup> and the unavoidable background levels of hydrogen in the ambient.<sup>106</sup> Recently, Schmidt et al.<sup>82</sup> demonstrated one of the first direct correlations between the approximate concentration of hydrogen and the LeTID-related defect concentration using a newly proposed method by Walter et al.<sup>107</sup> for hydrogen quantification. To achieve this, a set of FZ-Si wafers used for the hydrogen content measurements, and a set of mc-Si wafers used for LeTID concentration quantification, were processed in parallel and coated with SiN<sub>x</sub>:H films of varying Si:N ratios. The maximum LeTID concentration after degradation (120°C, 0.5 suns) on mc-Si wafers was then correlated with the bulk hydrogen concentration measured after H<sub>2</sub> dimer dissociation on the FZ-Si wafers (see Figure 12 and refer to further observations in Schmidt et al.<sup>82</sup>).

#### 4.2.2 | The influence of hydrogen from dielectric films

As mentioned earlier in Section 3.3, several studies have explored the impact of various dielectric films on LeTID degradation properties. Investigations have been conducted looking at the severity of LeTID in relation to the hydrogen both within and released from hydrogen containing dielectric films.<sup>54,59,108–110</sup> Using Fourier-transform infrared (FTIR) spectroscopy measurements, Vargas et al.<sup>54</sup> measured the fractional silicon-hydrogen (Si-H) and nitrogen-hydrogen (N-H) bond density within various SiN<sub>x</sub>:H films before and after contact firing at different temperatures. The released hydrogen fraction as reflected through diminishing bond densities after firing was compared with the LeTID defect density as illustrated in Figure 13A. Using a similar

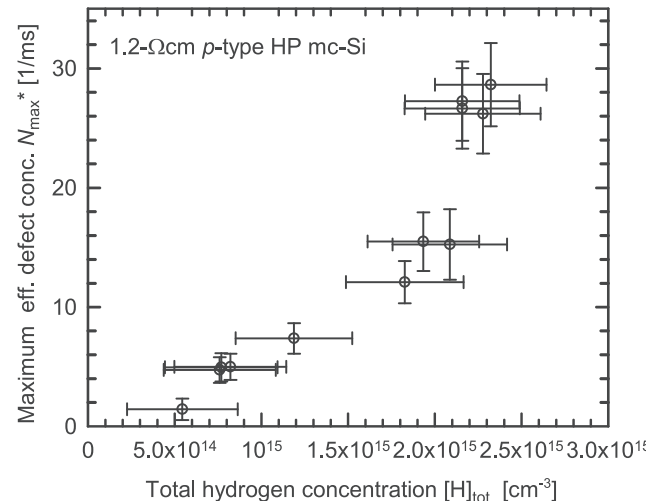


**FIGURE 12** Maximum effective defect concentrations  $N_{\text{max}}^*$  measured on neighbouring mc-Si sister wafers, which were coated on both surfaces with SiN<sub>x</sub>:H films of different Si:N ratios and fired at 900°C.  $N_{\text{max}}^*$  is plotted versus the total hydrogen content  $[H]_{\text{tot}}$  measured on boron-doped FZ-Si wafers, which were processed in parallel to the mc-Si wafers<sup>82</sup>

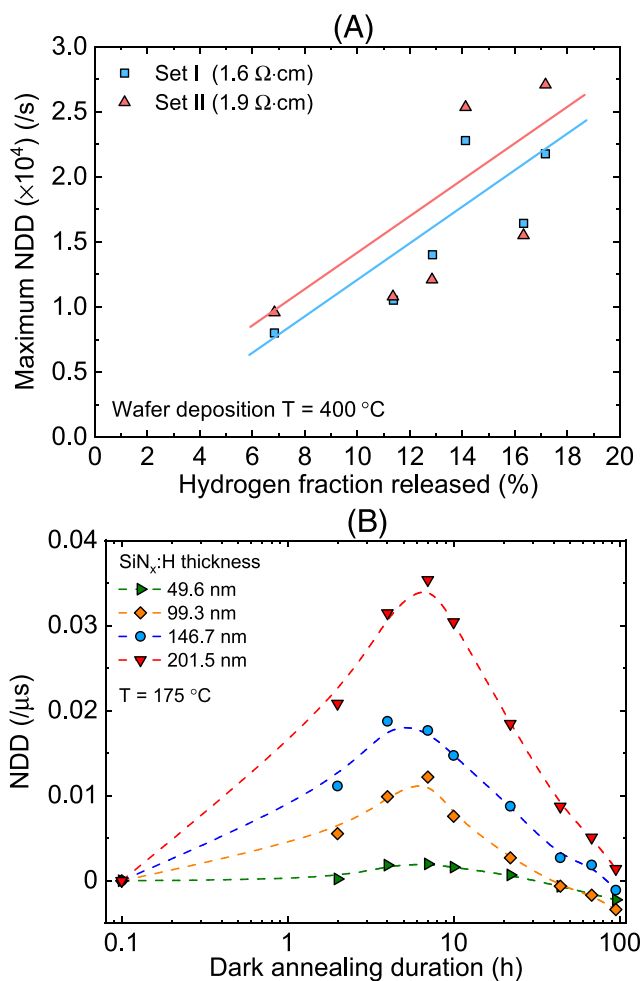


**FIGURE 13** (A) Maximum NDD as a function of the hydrogen fraction released for a  $\text{SiN}_x:\text{H}$  deposition temperature of  $400^\circ\text{C}$  on two sets of mc-Si materials. (B) Evolution of NDD versus dark annealing time at  $175^\circ\text{C}$  for mc-Si samples with varying  $\text{SiN}_x:\text{H}$  thicknesses. These figures are reproduced using data from the literature,<sup>54,111</sup> respectively

concept, we subsequently modulated the  $\text{SiN}_x:\text{H}$  film thickness and observed increasing maximum defect concentrations with increasing thicknesses, as depicted in Figure 13B. There, it was assumed that a higher volume of hydrogen within the passivation layers would lead to higher bulk hydrogen concentration.<sup>111</sup> The effect of  $\text{SiN}_x:\text{H}$  thickness on LeTID extent was confirmed by Bredemeier et al.,<sup>109</sup> where, in addition, a saturation in the LeTID extent was found for film thicknesses above 105 nm. Nevertheless, authors of the latter work pointed out that caution needs to be taken with some of the assumptions made in their work and that of Vargas et al., because using bulk boron-hydrogen (B-H) pair densities to calculate the total influx of hydrogen during firing showed that films of higher hydrogen content did not necessarily give rise to a greater bulk in-diffusion of hydrogen, suggesting that other film properties of the  $\text{SiN}_x:\text{H}$  layers may be the determinant of how much hydrogen is introduced to the silicon wafer.<sup>107</sup>

Indeed, as shown by Bredemeier et al.,<sup>109</sup> the  $\text{SiN}_x:\text{H}$  film atomic density, rather than the hydrogen concentration alone, greatly influences the hydrogen incorporation and the subsequent LeTID degradation extent. It may be that because N-rich films are expected to have a dense structure in contrast to Si-rich dielectrics with lower Si-N bond densities that atomic hydrogen in the latter would move more freely, either through effusion or out-diffusion processes. However, at lower atomic densities, hydrogen tends to form dimers, which again restrict bulk in-diffusion, resulting in a drop in bulk hydrogen concentration.

#### 4.2.3 | Other evidence for the involvement of hydrogen

In Fung et al.,<sup>112</sup> a series of isochronal annealing procedures were used to identify a relationship between LeTID and the formation and dissociation of hydrogen-boron complexes in a set of p-type mc-Si and Cz-Si wafers. A maximum in the LeTID-related defect density on mc-Si, and boron-oxygen defect passivation in Cz-Si was observed, both of which require the presence of hydrogen. This isochronal annealing behaviour was later correlated to the work by McQuaid et al.,<sup>113</sup> who showed using FTIR spectroscopy, a peak in the boron-hydrogen (B-H) pair concentrations with identical isochronal annealing durations and temperatures. It was thus concluded that although the majority of hydrogen after cofiring resides in a hydrogen dimer state ( $\text{H}_{2A}$ ) as described in Voronkov and Falster<sup>114</sup> and serves as a reservoir of hydrogen, thermal annealing allows for the dissociation of these dimers into a mobile interstitial form. The interactions between boron dopants and this hydrogen generates light-sensitive B-H pairs, which later dissociate under illuminated conditions to supply hydrogen for the formation of LeTID.

#### 4.2.4 | A concept of hydrogen-induced recombination

The prospect of hydrogen as a root cause has led to many theories regarding the recombination centre itself. A hypothesis was presented in Wenham et al.<sup>16</sup> which built upon the possible notion that large concentrations of hydrogen may cause recombination on its own. Coined hydrogen-induced recombination (HIR), this theory relies on the fermi-level dependence of hydrogen charge states in Herring et al.<sup>105</sup> and the nature of hydrogen in its ability to act as a dopant.<sup>115</sup> Hydrogen in various semiconductors, including silicon, is amphoteric in nature, that is, occurring in both positive and negative states. In p-type material, where there is an abundance of holes, hydrogen donates its electron and is stable in the positive charge state ( $\text{H}^+$ ). However, fundamentally, the dopant impurities that cause the material to be p-type in the first place (e.g., boron in p-type Si) are acceptors after contributing a hole to the valence band and reside in the negative state (e.g.,  $\text{B}_S^-$ ). By forces of coulombic attraction,  $\text{H}^+$  tends to neutralise and bind with the dopants (i.e., through forming neutral

$\text{BH}^0$ ). The reverse happens in n-type with an abundance of electrons; the hydrogen atom takes an electron, acting as an acceptor, and sits stably as ( $\text{H}^-$ ). It is thus, the inherent behaviour of hydrogen to counteract against the prevailing conductivity of the material in which it resides, a process known as 'counter-doping'. If hydrogen exists in silicon at concentrations above of the background doping concentration, it will counter-dope the silicon until the Fermi level is pinned at the  $\varepsilon(+/-)$  level in silicon. Under these conditions, any excess interstitial atomic hydrogen will have a maximum in the concentration of  $\text{H}^0$  and an equal probability of transitioning into  $\text{H}^+$  or  $\text{H}^-$ . Because  $\text{H}^0$  is thermodynamically unstable under equilibrium conditions with a lifetime in the order of nanoseconds, continuous transitions between  $\text{H}^-$  and  $\text{H}^+$  through  $\text{H}^0$  are required to preserve the equilibrium charge state fractions. According to our theory in,<sup>16</sup> the simultaneous loss of an electron ( $\text{H}^- - e^- \rightarrow \text{H}^0$ ) and a hole ( $\text{H}^+ - h^+ \rightarrow \text{H}^0$ ) by  $\text{H}^-$  and  $\text{H}^+$  provides the constituents to a recombination event. The details of this theory can be found in other studies.<sup>16,116</sup> Interestingly, Nickel et al.<sup>117</sup> noted that the conditions described here are conducive to hydrogen platelet formation, that is, when hydrogen concentrations exceed  $>10^{17} \text{ cm}^{-3}$  and the fermi-level crosses hydrogen's  $\varepsilon(+/-)$  level, the existence of  $\text{H}^+$  and  $\text{H}^-$  in the same locality causes the hydrogen to attack the lattice  $\varepsilon(+/-)$  level, forming structural defects.

Results that would appear to contradict the theory that hydrogen itself causes LeTID were presented by Jensen et al.<sup>98</sup> (refer back to Section 4.2.1). In that study, it was reported that the firing process itself does not cause LeTID and hydrogen is required for LeTID to occur. The finding that samples fired (in the absence of hydrogen containing films) before hydrogen introduction (via MIRHP) did not degrade, led to the conclusion that two reactants are required—hydrogen and one or more defects that can be modified separately by firing. In addition, the solubility of interstitial hydrogen in silicon makes it very unlikely for the conditions required for complete dopant compensation—usually requiring hydrogen concentrations far exceeding the dopant concentration—to exist within the bulk at low temperature.

### 4.3 | Prospects for future work

At this point in time, it is difficult to rule out the involvement of all metallic impurities, nonmetals or a theory of hydrogen on its own. Little is currently understood with regard to the exact composition or configuration of the defect. Measurements by Chunlan et al.<sup>24</sup> and Mchedlidze et al.<sup>64</sup> using DLTS have provided some insight into what the defect may be. Chunlan et al.<sup>24</sup> reported two traps in degraded p-type mc-Si PERC cells with deep energy levels of  $E_V + 0.485\text{eV}$  associated with an interstitial iron ( $\text{Fe}_i$ ) complex and  $E_V + 0.295 \text{ eV}$  associated with iron-hydrogen ( $\text{Fe}-\text{H}$ ) pairs. Due to the metastable nature of  $\text{Fe}_i$  in silicon and overlaps in activation energy extracted from the DLTS spectra, the authors could not, however, exclude the contributions of other transition metals. Similarly, also on p-type mc-Si PERC solar cells, Mchedlidze et al.<sup>64</sup> obtained two minority carrier traps with energy levels located at  $E_C - 0.19 \text{ eV}$  and  $E_C - 0.34 \text{ eV}$ .

It was concluded that the defects responsible for the degradation were likely formed near structural defects in the bulk of the silicon and have an intrinsic origin; however, the exact species could not be determined. From these studies, it would be useful to consider future DLTS analysis to be carried out on LeTID-susceptible FZ-Si wafers where the impact of crystallographic defects and metallic impurities may be largely excluded.

## 5 | MITIGATION OF LETID

Finding commercial solutions for LeTID defect suppression and mitigation has been of critical importance to the PV industry as it has transitioned towards PERC. Numerous techniques have been reported in the literature, either as changes to the fabrication steps of the solar cell or as additional post-processing steps on finished solar cells. These will be described here in the order in which they could be applied during the cell fabrication process. From a starting material perspective, LeTID extent reduces with wafer thickness<sup>83</sup> and thus, using thinner wafers could be one approach to reducing LeTID in solar cells. Reduction of wafer thickness, however, potentially raises yield and handling concerns, particularly for screen-printed solar cells.<sup>118</sup> It has also been shown that wafer selection can play an important role in the LeTID extent of solar cells.<sup>26</sup> Wafers from different ingots, or even the same ingot<sup>3,7</sup> can show vastly different LeTID characteristics, and thus selecting wafers with lower LeTID potential is one method for reducing LeTID in finished solar cells. Nonetheless, in reference to p-type mc-Si wafers, it was noted in a study by Hanwha Q Cells that there were 'no LeTID free wafers found on the market'.<sup>3</sup> It is also desirable for a solar cell manufacturer to be able to use the entire ingot for solar cell production and to not have to screen for LeTID at a wafer level.

Based on the observations that a phosphorus gettering process can reduce LeTID,<sup>93,94</sup> it is likely that optimisation of the emitter diffusion process during cell production can help to suppress LeTID. As also discussed in Section 4.2.2, dielectric layer composition,<sup>54,82,119</sup> thickness<sup>83,111</sup> and stoichiometry<sup>109</sup> has been shown to have a significant impact on LeTID, likely due to the modulation of hydrogen diffusion into the silicon bulk associated with the changes in the films. Bredemeier et al.<sup>109</sup> identified that a  $\text{SiN}_x:\text{H}$  refractive index (RI) of below 1.9 or above 3 resulted in reduced LeTID. Tuning of  $\text{SiN}_x:\text{H}$  to avoid LeTID will have impacts on the solar cell electrical and optical performance that need to be considered. Changes in film hardness can alter the penetration depth of the Ag fingers during metallization, leading to shunting or poor ohmic contact, thus cofiring would need to be reoptimized with this approach. Changes in dielectric thickness will reduce the anti-reflective behaviours for certain wavelengths of light. Furthermore, although silicon-rich  $\text{SiN}_x:\text{H}$  films (high RI) can provide better surface passivation they are usually absorptive in the short and medium wavelength range leading to parasitic losses.<sup>120</sup> Another obvious method for suppressing LeTID is through the modification of the metallization firing profile. In the work by Nakayashiki et al., Bredemeier et al. and Chan et al., it was reported that the degradation

could be suppressed by reducing the cell or wafer firing temperature. In the case of Nakayashiki et al., this method of LeTID suppression was demonstrated on finished solar cells incorporated into a module, with significantly reduced power loss after 50 days of outdoor soaking (8% reduced to 3% for 960°C and 860°C firing temperatures, respectively). While reducing the firing temperature much further than this is likely not compatible with current screen-print pastes, Eberle et al. demonstrated that the LeTID defect could be suppressed even at higher peak firing temperatures if the cooling rate were slowed. In that study, using a rapid thermal processor (RTP) with a slower cooling rate, LeTID was effectively suppressed even at a high peak firing temperature of 800°C. This study was carried out on lifetime samples, and when applied to actual solar cells, would need to be carefully optimised for the front ohmic contacts and appropriate formation of rear Al-BSF regions.

Several postprocessing methods have been introduced to suppress LeTID, all of which involve annealing of the finished solar cell either under illumination,<sup>14,15,17,20</sup> with current injection<sup>2,15,121</sup> or in darkness,<sup>41,73,88,122</sup> demonstrating that there are likely two paths to mitigating the LeTID defect, through the injection of carriers at elevated temperatures and through a purely thermal route. Annealing under laser illumination to accelerate the degradation and regeneration process was proposed by both Payne et al. and Krauß et al., in an approach similar to that proposed for rapid mitigation of the BO defect in the past.<sup>123–125</sup> As LeTID is a CID mechanism, an equivalent process can also be performed in the dark while injecting current into the cell, however the carrier densities achievable during this process are significantly lower than what can be achieved by high intensity illumination, thus a current injection LeTID mitigation process is generally slower. Annealing a finished cell in a belt firing furnace or 're-firing' is another approach that has been shown to effectively suppress LeTID, although this method can be detrimental to device series resistances ( $R_s$ ) if not carefully optimised.<sup>14,20,126</sup> Peral et al. attributed this observed increase in  $R_s$  with extended contact firing to a thickening of the glass layer surrounding the silver crystallites within the metal contact, thus inducing resistance against current flow.<sup>126</sup> Annealing in the dark has also been shown to suppress LeTID.<sup>41,73,88</sup> Similar to the approach in the belt-furnace, dark annealing has been shown to result in a drop in device FF for longer durations and higher temperatures.<sup>122</sup> To avoid the drop in device FF, Sen et al.<sup>127</sup> proposed a possible alternative method whereby the anneal is performed prior to metal contact firing. This approach has shown to be effective on lifetime test structures but has yet to be demonstrated on cells, and the effect of changes in density of the  $\text{SiN}_x\text{-H}$  layer after annealing on the cofiring process may need to be considered. In an alternative approach to avoid the FF increase, Hamer et al.<sup>122</sup> proposed annealing the cell in the dark with a reverse bias voltage applied. In this approach, it is hypothesised that the electric field repels hydrogen from the metal/Si contact interface that would otherwise be responsible for the drop in FF. A summary of the various mitigation strategies presented throughout the literature is presented in Table 3.

Several commercial tools to treat LeTID have emerged into the market. These include illuminated annealing tools: laser based

**TABLE 3** Summary of various suppression or mitigation strategies at a wafer or cell level as highlighted throughout the literature

| Source                           | Treatment  |
|----------------------------------|--|
| Bredemeier et al. <sup>83</sup>  | Reducing the thickness of the silicon wafer resulting in a supposed faster diffusion of impurities to the surface  |
| Zuschlag et al. <sup>93</sup>    | Use of phosphorus diffusion gettering (PDG) to suppress LeTID  |
| Skorka et al. <sup>94,128</sup>  | Use of phosphorus diffusion gettering (PDG) to suppress LeTID  |
| Chakraborty et al. <sup>95</sup> | Use of phosphorus diffusion gettering (PDG) to suppress LeTID  |
| Eberle et al. <sup>35</sup>      | Reduction of the cooling rate during firing using an RTP furnace   |
| Chan et al. <sup>14</sup>        | Secondary post metallization firing process (480°C–660°C) + laser processing (200°C, >40 suns)   |
| Sen et al. <sup>78</sup>         | Reduction of the cooling rate during firing using an RTP furnace   |
| Bredemeier et al. <sup>129</sup> | Post-firing anneals in a commercial in-line furnace-based tool (c.REG)   |
| Sen et al. <sup>127</sup>        | Low temperature annealing (~650°C) prior to metallization firing to suppress the issues associated with increased FF   |
| Sen et al. <sup>20</sup>         | Application of a two-step moderate temperature annealing process post-metallization firing in a belt furnace.  |
| Sharma et al. <sup>41</sup>      | Optimisation of firing conditions with reductions in peak firing temperature and modification of belt speed. Use of post metallization dark annealing at moderate temperatures (300°C–550°C) |
| Sharma et al. <sup>130</sup>     | Incorporation of postfiring forming gas annealing (FGA)  |
| Yli-koski et al. <sup>131</sup>  | Application of a low-temperature (200°C–300°C) long duration (>18.5 h) anneal to suppress subsequent LeTID formation   |
| Varshney et al. <sup>111</sup>   | Reductions in the thickness of $\text{SiN}_x$ films to reduce in-diffused hydrogen content   |
| Varshney et al. <sup>132</sup>   | Implementation of ALD deposited $\text{Al}_2\text{O}_3$ films as a blocking layer for hydrogen in-diffusion during firing  |
| Bredemeier et al. <sup>109</sup> | Tuning of $\text{SiN}_x$ films to high (towards 3) or low (towards 1.9) refractive indexes to reduce hydrogen mobility or density, respectively  |
| Payne et al. <sup>8,15</sup>     | High intensity laser (44.8 kW/m <sup>2</sup> ) and high temperature process (140°C) to accelerate defect formation and recovery rates  |
| Wang et al. <sup>121</sup>       | Use of single or double current injection annealing (CIA) processes (260°C, 14.5 A) on finished solar cells  |

(Figure 14A),<sup>133</sup> LED-based, modified metallization furnace-based tools (Figure 14B)<sup>129</sup> and dark annealing tools involving the injection of current (Figure 14C).<sup>121</sup> The latter has seen wide adoption by the industry due to the increased throughput of the batch 'coin stack' technique that is compatible with this process in addition to a typically smaller production line footprint.

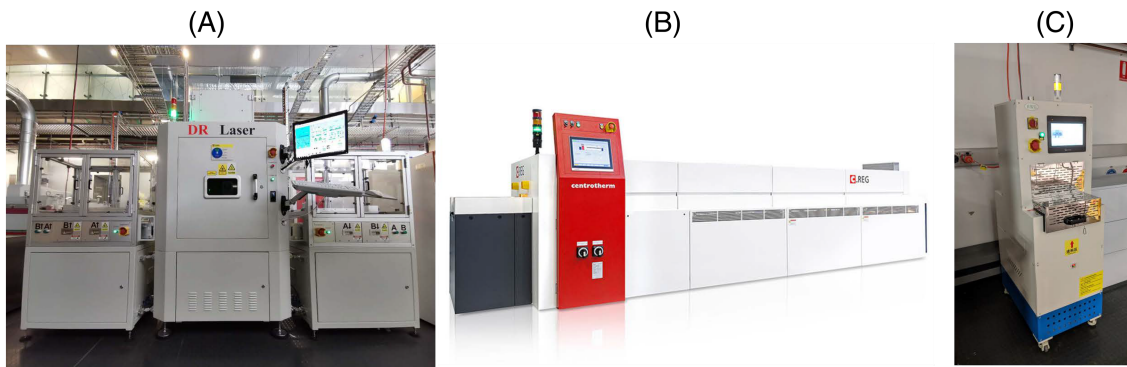


**FIGURE 14** A commercial (A) laser-based LeTID and LID mitigation tool (*DR Laser*), (B) in-line modified regeneration furnace (c.REG, *Centrotherm International*)<sup>129</sup> and (C) coin-stack current injection tool

It may seem that from the many LeTID mitigation methods discussed above that there can be a tendency, in one way or the other, to opt for the reduction in total hydrogen concentrations within the bulk of the solar cells.<sup>134</sup> However, it is important to highlight the detrimental effects that this approach may represent. Hydrogen is recognised as being essential for the passivation of bulk defects, particularly in mc-Si wafers for grain boundaries and other structural defects, and in Cz-Si wafers for the passivation of BO defects as discussed in previous works.<sup>135,136</sup> It is therefore crucial to strike a balance between removing excess hydrogen that may lead to LeTID, while maintaining sufficient hydrogen concentrations for the passivation of other defects including the one responsible for BO-LID.

## 6 | CONCLUSION

Although there has been sustained research into LeTID for nearly a decade, the specific recombination-active defect remains unknown. Nevertheless, there has been significant progress in understanding the properties and behaviour of the defect and perhaps most importantly, industrially applicable methods for mitigation. Over the years, numerous studies have helped to elucidate properties and behaviour of the defect: It is firing-dependent; it can be present in all types of silicon wafers; it is dependent on the dielectric passivating layers present during firing; it can be activated by illumination or current-injection at elevated temperatures, or simply through annealing in the dark. Several hypotheses have been put forward regarding the defect composition: metallic impurities, hydrogen or a combination of both. Regardless of the exact nature of the defect, a consensus has formed on hydrogen playing an important role in the degradation, with a vast amount of experimental evidence pointing towards its involvement in LeTID. Although LeTID still remains a concern for the silicon PV industry, the innovations developed by industry and academia over the last decade have greatly reduced the severity of the problem, particularly for mc-Si PERC cells, being the most susceptible to LeTID. Through material selection, process adaptation and post-cell fabrication steps, solar cell manufacturers have been

able to suppress LeTID in these cells from the typically reported 10%–12% relative efficiency loss to less than 2% relative. Ongoing investigation into the exact nature and composition of the defect is likely required to fully eliminate this problem.

## FUNDING INFORMATION

This work was supported by the Australian Centre for Advanced Photovoltaics (ACAP), grant numbers RG200768-C, 1-SRI001 and RG200768-B; the Australian Government Research Training Program: RSAP1000; the Australian Research Council (ARC), award number: DE170100620; the Australian Renewable Energy Agency (ARENA): 1-A060, RND005 and RND010; the Institution of Engineering and Technology: AF Harvey Engineering Prize; and the National Science Foundation and the Department of Energy Cooperative Agreement: No. EEC-1041895.

## ACKNOWLEDGEMENTS

The authors would like to dedicate this work to the late Professor Stuart Wenham (15 July 1957–23 December 2017) for his dedication and contributions to photovoltaics around the world. The views expressed herein are not necessarily the views of the Australian Government, and the Australian Government does not accept responsibility for any information or advice contained herein. The authors would also like to acknowledge the UNSW Hydrogenation Team for the avid discussions, Dr. Matthew Wright for all the additional help and support in proofing this manuscript as well as the international photovoltaic community for their research and contributions into understanding LeTID.

## ORCID

Daniel Chen  <https://orcid.org/0000-0001-7379-4751>

Michelle Vaqueiro Contreras  <https://orcid.org/0000-0002-6770-5780>

Alison Ciesla  <https://orcid.org/0000-0002-5109-6458>

Phillip Hamer  <https://orcid.org/0000-0003-2168-4053>

Brett Hallam  <https://orcid.org/0000-0002-4811-5240>

Catherine Chan  <https://orcid.org/0000-0003-4327-1081>

## REFERENCES

- Ramspeck K, Zimmermann S, Nagel H, et al. Light induced degradation of rear passivated mc-Si solar cells, in: Proc. 27th Eur. Photovolt. Sol. Energy Conf., 2012: pp. 861–865. <https://doi.org/10.4229/27THEUPSEC2012-2DO.3.4>
- Kersten F, Engelhart P, Ploigt H-C, et al. Degradation of multi-crystalline silicon solar cells and modules after illumination at elevated temperature. *Sol Energy Mater sol Cells.* 2015;142:83–86. <https://doi.org/10.1016/j.solmat.2015.06.015>
- Petter K, Hubener K, Kersten F, et al. Dependence of LeTID on brick height for different wafer suppliers with several resistivities and dopants, 9th Int. Work Cryst Silicon Sol Cells. 2016.
- Fertig F, Broisch J, Biro D, Rein S. Stability of the regeneration of the boron-oxygen complex in silicon solar cells during module certification. *Sol Energy Mater sol Cells.* 2014;121:157–162. <https://doi.org/10.1016/j.solmat.2013.10.014>
- Lee K, Kim M, Lim J, Ahn J, Hwang M, Cho E. Natural recovery from LID: regeneration under field conditions?, in: 31st Eur. Photovolt. Sol. Energy Conf. Exhib., 2015: pp. 1835–1837. <https://doi.org/10.4229/EUPVSEC20152015-5CO.16.6>
- Kersten F, Fertig F, Petter K, et al. System performance loss due to LeTID, in: Energy Procedia, 2017: pp. 540–546. <https://doi.org/10.1016/j.egypro.2017.09.260>
- Kersten F, Engelhart P, Ploigt HC, et al. A new mc-Si degradation effect called LeTID, 2015 IEEE 42nd Photovolt. Spec Conf PVSC 2015. 2015. <https://doi.org/10.1109/PVSC.2015.7355684>
- Payne DNR, Chan CE, Hallam BJ, et al. Acceleration and mitigation of carrier-induced degradation in p-type multi-crystalline silicon. *Phys Status Solidi Rapid Res Lett.* 2016;10:237–241. <https://doi.org/10.1002/pssr.201510437>
- Lindroos J, Savin H. Review of light-induced degradation in crystalline silicon solar cells. *Sol Energy Mater sol Cells.* 2016;147:115–126. <https://doi.org/10.1016/j.solmat.2015.11.047>
- Inglese A, Lindroos J, Vahlman H, Savin H. Recombination activity of light-activated copper defects in p-type silicon studied by injection- and temperature-dependent lifetime spectroscopy. *J Appl Phys.* 2016;120:125703. <https://doi.org/10.1063/1.4963121>
- Luka T, Großer S, Hagendorf C, Ramspeck K, Turek M. Intra-grain versus grain boundary degradation due to illumination and annealing behavior of multi-crystalline solar cells. *Sol Energy Mater sol Cells.* 2016;158:43–49. <https://doi.org/10.1016/j.solmat.2016.05.061>
- Niewelt T, Selinger M, Grant NE, Kwaplil W, Murphy JD, Schubert MC. Light-induced activation and deactivation of bulk defects in boron-doped float-zone silicon. *J Appl Phys.* 2017;121:185702. <https://doi.org/10.1063/1.4983024>
- Vargas C, Zhu Y, Coletti G, et al. Recombination parameters of lifetime-limiting carrier-induced defects in multicrystalline silicon for solar cells. *Appl Phys Lett.* 2017;110:092106. <https://doi.org/10.1063/1.4977906>
- Chan CE, Payne DNR, Hallam BJ, et al. Rapid stabilization of high-performance multicrystalline p-type silicon PERC cells. *IEEE J Photovolta.* 2016;6:1473–1479. <https://doi.org/10.1109/JPHOTOV.2016.2606704>
- Payne DNR, Chan CE, Hallam BJ, et al. Rapid passivation of carrier-induced defects in p-type multi-crystalline silicon. *Sol Energy Mater sol Cells.* 2016;158:102–106. <https://doi.org/10.1016/j.solmat.2016.05.022>
- Wenham ACN, Wenham S, Chen R, et al. Hydrogen-induced degradation, in: 2018 IEEE 7th World Conf. Photovolt. Energy Conversion, WCPEC 2018 - A Jt. Conf. 45th IEEE PVSC, 28th PVSEC 34th EU PVSEC, IEEE, 2018: pp. 1–8. <https://doi.org/10.1109/PVSC.2018.8548100>
- Kraus K, Brand AA, Fertig F, Rein S, Nekarda J. Fast regeneration processes to avoid light-induced degradation in multicrystalline silicon solar cells. *IEEE J Photovolt.* 2016;6:1427–1431. <https://doi.org/10.1109/JPHOTOV.2016.2598273>
- Luka T, Eiternick S, Frigge S, Hagendorf C, Mehlich H, Turek M. Investigation of light induced degradation of multi-crystalline PERC cells, 31st Eur. Photovolt Sol Energy Conf Exhib. 2015:826–828.
- Sen C, Chan C, Chen D, et al. Different extent and behaviour of LeTID in the past and current PERC silicon solar cells. *Asia-Pacific sol Res Conf.* 2020;2:3–6.
- Sen C, Chan C, Hamer P, et al. Eliminating light- and elevated temperature-induced degradation in p-type PERC solar cells by a two-step thermal process. *Sol Energy Mater sol Cells.* 2020;209:110470. <https://doi.org/10.1016/j.solmat.2020.110470>
- Deniz H, Bauer J, Breitenstein O. Nickel precipitation in light and elevated temperature degraded multicrystalline silicon solar cells. *Sol RRL.* 2018;2:1800170. <https://doi.org/10.1002/solr.201800170>
- Sio HC, Wang H, Wang Q, et al. Light and elevated temperature induced degradation in p-type and n-type cast-grown multi-crystalline and mono-like silicon. *Sol Energy Mater sol Cells.* 2018;182:98–104. <https://doi.org/10.1016/j.solmat.2018.03.002>
- Padmanabhan M, Jhaveri K, Sharma R, et al. Light-induced degradation and regeneration of multicrystalline silicon Al-BSF and PERC solar cells. *Phys Status Solidi Rapid Res Lett.* 2016;10:874–881. <https://doi.org/10.1002/pssr.201600173>
- Zhou C, Zhou S, Ji F, Wang W. Deep level transient spectroscopic investigation of carrier trap defects in p-type mc-Si PERC solar cells after elevated temperature light soaking, 36th Eur. Photovolt. Sol. Energy Conf. Exhib. 2019:147–150. <https://doi.org/10.4229/EUPVSEC20192019-2BO.1.2>
- Fertig F, Krauß K, Rein S. Light-induced degradation of PECVD aluminium oxide passivated silicon solar cells. *Phys Status Solidi Rapid Res Lett.* 2015;9:41–46. <https://doi.org/10.1002/pssr.201409424>
- Nakayashiki K, Hofstetter J, Morishige AE, et al. Engineering solutions and root-cause analysis for light-induced degradation in p-type multicrystalline silicon PERC modules. *IEEE J Photovolta.* 2016;6:860–868. <https://doi.org/10.1109/JPHOTOV.2016.2556981>
- Fokuhl E, Naeem T, Schmid A, Gebhardt P, Geipel T, Philipp D. LeTID—a comparison of test methods on module level, in: 36th Eur. PV Sol. Energy Conf. Exhib., 2019: pp. 75–84. <https://doi.org/10.1037/0033-2909.I26.1.78>
- Pander M, Luka T, Jäckel B, et al. Prediction of potential power/yield loss from LeTID susceptible, 36th Eur. Photovolt. Sol. Energy Conf. Exhib. 2019:810–815. <https://doi.org/10.4229/EUPVSEC20192019-4BO.12.1>
- Terrestrial photovoltaic (PV) modules—design qualification and type approval—part 2: test procedures, IEC 61215–2 ED2. 2018.
- Measurement of light-induced degradation of crystalline silicon photovoltaic cells, IEC 63202–1. 2020.
- Repins IL, Kersten F, Hallam B, VanSant K, Koentopp MB. Stabilization of light-induced effects in Si modules for IEC 61215 design qualification. *Sol Energy.* 2020;208:894–904. <https://doi.org/10.1016/j.solener.2020.08.025>
- Sperber D, Heilemann A, Herguth A, Hahn G. Temperature and light-induced changes in bulk and passivation quality of boron-doped float-zone silicon coated with SiNx:H. *IEEE J Photovolta.* 2017;7:463–470. <https://doi.org/10.1109/JPHOTOV.2017.2649601>
- Keller P. Untersuchung und Wasserstoffpassivierung von Defekten in Foliensilizium und multikristallinen Silizium-Materialien (investigation and hydrogen passivation of defects in foil silicon and multicrystalline silicon materials), Univ. Konstanz Thesis. 2017.
- Bredemeier D, Walter D, Herlufsen S, Schmidt J. Lifetime degradation and regeneration in multicrystalline silicon under illumination at elevated temperature. *AIP Adv.* 2016;6:035119. <https://doi.org/10.1063/1.4944839>

35. Eberle R, Kwapił W, Schindler F, Schubert MC, Glunz SW. Impact of the firing temperature profile on light induced degradation of multi-crystalline silicon. *Phys Status Solidi Rapid Res Lett.* 2016;865:861-865. <https://doi.org/10.1002/pssr.201600272>
36. Chen D, Kim M, Stefani BV, et al. Evidence of an identical firing-activated carrier-induced defect in monocrystalline and multi-crystalline silicon. *Sol Energy Mater sol Cells.* 2017;172:293-300. <https://doi.org/10.1016/j.solmat.2017.08.003>
37. Chen D, Hamer PG, Kim M, et al. Hydrogen induced degradation: a possible mechanism for light- and elevated temperature-induced degradation in n-type silicon. *Sol Energy Mater sol Cells.* 2018;185: 174-182. <https://doi.org/10.1016/j.solmat.2018.05.034>
38. Bredemeier D, Walter D, Herlufsen S, Schmidt J. Understanding the light-induced lifetime degradation and regeneration in multi-crystalline silicon. *Energy Procedia.* 2016;92:773-778. <https://doi.org/10.1016/j.egypro.2016.07.060>
39. Chung D, Chan C, Mitchell B, Altermatt PP, Trupke T, Abbott M. Effect of wafer position in ingot on the light and elevated temperature induced degradation (LeTID) of multicrystalline silicon, in: 2018 IEEE 7th World Conf. Photovolt. Energy Convers. (A Jt. Conf. 45th IEEE PVSC, 28th PVSEC 34th EU PVSEC), IEEE, 2018: pp. 303-308. <https://doi.org/10.1109/PVSC.2018.8547497>
40. Herguth A, Keller P, Mundhaas N. Influence of temperature on light induced phenomena in multicrystalline silicon, in: AIP Conf. Proc., 2018: p. 130007. <https://doi.org/10.1063/1.5049326>
41. Sharma R, Aberle AG, Li JB. Optimization of belt furnace anneal to reduce light and elevated temperature induced degradation of effective carrier lifetime of p-type multicrystalline silicon wafers. *Sol RRL.* 2018;2:1800070. <https://doi.org/10.1002/solr.201800070>
42. Kim M, Wenham S, Unsur V, Ebong A, Hallam B. Impact of rapid firing thermal processes on meta-stable defects: preformation of the LeTID and the suppression of B-O defects, in: 2018 IEEE 7th World Conf. Photovolt. Energy Conversion, WCPEC 2018 - A Jt. Conf. 45th IEEE PVSC, 28th PVSEC 34th EU PVSEC, 2018: pp. 341-346. <https://doi.org/10.1109/PVSC.2018.8547666>
43. Fritz JM, Zuschlag A, Skorka D, Schmid A, Hahn G. Temperature dependent degradation and regeneration of differently doped mc-Si materials. *Energy Procedia.* 2017;124:718-725. <https://doi.org/10.1016/j.egypro.2017.09.085>
44. Liu S, Payne D, Vargas Castrillon C, et al. Impact of dark annealing on the kinetics of light- and elevated-temperature-induced degradation. *IEEE J Photovolt.* 2018;8:1494-1502. <https://doi.org/10.1109/JPHOTOV.2018.2866325>
45. Vargas C, Nie S, Chen D, et al. Degradation and recovery of n-type multi-crystalline silicon under illuminated and dark annealing conditions at moderate temperatures. *IEEE J Photovolt.* 2019;9:355-363. <https://doi.org/10.1109/JPHOTOV.2018.2885711>
46. Niewelt T, Post R, Schindler F, Kwapił W, Schubert MC. Investigation of LeTID where we can control it—Application of FZ silicon for defect studies, in: 15th Int. Conf Conc Photovolt Syst, 2019: p. 140006. <https://doi.org/10.1063/1.5123893>
47. Krauss K, Fertig F, Menzel D, Rein S. Light-induced degradation of silicon solar cells with aluminiumoxide passivated rear side. *Energy Procedia.* 2015;77:599-606. <https://doi.org/10.1016/j.egypro.2015.07.086>
48. Fertig F, Lantzsch R, Mohr A, et al. Mass production of p-type Cz silicon solar cells approaching average stable conversion efficiencies of 22%, in: Energy Procedia, 2017: pp. 338-345. <https://doi.org/10.1016/j.egypro.2017.09.308>
49. Grant NE, Scowcroft JR, Pointon AI, Al-Amin M, Altermatt PP, Murphy JD. Lifetime instabilities in gallium doped monocrystalline PERC silicon solar cells. *Sol Energy Mater sol Cells.* 2020;206:110299. <https://doi.org/10.1016/j.solmat.2019.110299>
50. Singha B, Solanki CS. N-type solar cells: advantages, issues, and current scenarios. *Mater Res Express.* 2017;4:072001. <https://doi.org/10.1088/2053-1591/aa6402>
51. Chen D, Hamer P, Kim M, et al. Hydrogen-induced degradation: explaining the mechanism behind light- and elevated temperature-induced degradation in n- and p-type silicon. *Sol Energy Mater sol Cells.* 2020;207:110353. <https://doi.org/10.1016/j.solmat.2019.110353>
52. Renevier C, Fourmond E, Forster M, Parola S, Le Coz M, Picard E. Lifetime degradation on n-type wafers with boron-diffused and SiO<sub>2</sub>/SiN-passivated surface. *Energy Procedia.* 2014;55:280-286. <https://doi.org/10.1016/j.egypro.2014.08.082>
53. Phang SP, Macdonald D. Direct comparison of boron, phosphorus, and aluminum gettering of iron in crystalline silicon. *J Appl Phys.* 2011;109:073521. <https://doi.org/10.1063/1.3569890>
54. Vargas C, Kim K, Coletti G, et al. Carrier-induced degradation in multicrystalline silicon: dependence on the silicon nitride passivation layer and hydrogen released during firing. *IEEE J Photovolt.* 2018;8:413-420. <https://doi.org/10.1109/JPHOTOV.2017.2783851>
55. Sperber D, Schwarz A, Herguth A, Hahn G. Bulk and surface-related degradation in lifetime samples made of Czochralski silicon passivated by plasma-enhanced chemical vapor deposited layer stacks. *Phys Status Solidi.* 2018;215:1800741. <https://doi.org/10.1002/pssa.201800741>
56. Sperber D, Furtwängler F, Herguth A, Hahn G. Does LeTID occur in c-Si even without a firing step?, in: AIP Conf. Proc., 2019: p. 140011. <https://doi.org/10.1063/1.5123898>
57. Kersten F, Heitmann J, Müller JW. Influence of Al<sub>2</sub>O<sub>3</sub> and SiN<sub>x</sub> passivation layers on LeTID. *Energy Procedia.* 2016;92:828-832. <https://doi.org/10.1016/j.egypro.2016.07.079>
58. Kersten F, Forster I, Peters S. Evaluation of spatial ALD of Al<sub>2</sub>O<sub>3</sub> for rear surface passivation of mc-Si PERC solar cells, 32nd Eur. Photovoltaic. Sol. Energy Conf. Exhib. 2016. <https://doi.org/10.4229/eupvsec20162016>
59. Varshney U, Abbott MD, Liu S, et al. Influence of dielectric passivation layer thickness on LeTID in multicrystalline silicon, in: 2018 IEEE 7th World Conf. Photovolt. Energy Convers. (A Jt. Conf. 45th IEEE PVSC, 28th PVSEC 34th EU PVSEC), IEEE, 2018: pp. 363-367. <https://doi.org/10.1109/PVSC.2018.8547618>
60. Selinger M, Kwapił W, Schindler F, et al. Spatially resolved analysis of light induced degradation of multicrystalline PERC solar cells. *Energy Procedia.* 2016;92:867-872. <https://doi.org/10.1016/j.egypro.2016.07.095>
61. Jensen MA, Morishige AE, Chakraborty S, et al. Do grain boundaries matter? Electrical and elemental identification at grain boundaries in LeTID-affected p-type multicrystalline silicon, in: 2017 IEEE 44th Photovolt. Spec. Conf., IEEE, 2017: pp. 3300-3303. <https://doi.org/10.1109/PVSC.2017.8366779>
62. Niewelt T, Schindler F, Kwapił W, Eberle R, Schön J, Schubert MC. Understanding the light-induced degradation at elevated temperatures: similarities between multicrystalline and floatzone p-type silicon. *Prog Photovolt Res Appl.* 2018;26:533-542. <https://doi.org/10.1002/pip.2954>
63. Lindroos J, Zuschlag A, Carstensen J, Hahn G. Light-induced degradation variation in industrial multicrystalline PERC silicon solar cells, AIP Conf Proc 1999. 2018. <https://doi.org/10.1063/1.5049332>
64. Mchedlidze T, Weber J. Location and properties of carrier traps in mc-Si solar cells subjected to degradation at elevated temperatures. *Phys Status Solidi.* 2019;216:1900142. <https://doi.org/10.1002/pssa.201900142>
65. Lim SY, Forster M, Zhang X, et al. Applications of photoluminescence imaging to dopant and carrier concentration measurements of silicon wafers. *IEEE J Photovolt.* 2013;3:649-655. <https://doi.org/10.1109/JPHOTOV.2013.6500013>

- doi.org/10.1109/JPHOTOV.2012.2228301
- 66. Sperber D, Herguth A, Hahn G. A 3-state defect model for light-induced degradation in boron-doped float-zone silicon. *Phys Status Solidi Rapid Res Lett.* 2017;11:1600408. <https://doi.org/10.1002/pssr.201600408>
  - 67. Kwapl W, Niewelt T, Schubert MC. Kinetics of carrier-induced degradation at elevated temperature in multicrystalline silicon solar cells. *Sol Energy Mater sol Cells.* 2017;173:80-84. <https://doi.org/10.1016/j.solmat.2017.05.066>
  - 68. Bredemeier D, Walter D, Schmidt J. Light-induced lifetime degradation in high-performance multicrystalline silicon: detailed kinetics of the defect activation. *Sol Energy Mater sol Cells.* 2017;173:2-5. <https://doi.org/10.1016/j.solmat.2017.08.007>
  - 69. Fung TH, Kim M, Chen D, et al. A four-state kinetic model for the carrier-induced degradation in multicrystalline silicon: introducing the reservoir state. *Sol Energy Mater sol Cells.* 2018;184:48-56. <https://doi.org/10.1016/j.solmat.2018.04.024>
  - 70. Bothe K, Schmidt J. Electronically activated boron-oxygen-related recombination centers in crystalline silicon. *J Appl Phys.* 2006;99:013701. <https://doi.org/10.1063/1.2140584>
  - 71. Kim K, Chen R, Chen D, et al. Degradation of surface passivation and bulk in p-type monocrystalline silicon wafers at elevated temperature. *IEEE J Photovolt.* 2019;9:97-105. <https://doi.org/10.1109/JPHOTOV.2018.2878791>
  - 72. Luka T, Turek M, Hagendorf C. Defect formation under high temperature dark-annealing compared to elevated temperature light soaking. *Sol Energy Mater sol Cells.* 2018;187:194-198. <https://doi.org/10.1016/j.solmat.2018.06.043>
  - 73. Chan C, Fung TH, Abbott M, et al. Modulation of carrier-induced defect kinetics in multi-crystalline silicon PERC cells through dark annealing. *Sol RRL.* 2017;1:1600028. <https://doi.org/10.1002/solr.201600028>
  - 74. Schmidt J. Temperature- and injection-dependent lifetime spectroscopy for the characterization of defect centers in semiconductors. *Appl Phys Lett.* 2003;82:2178-2180. <https://doi.org/10.1063/1.1563830>
  - 75. Nampalli N. Characterisation and passivation of boron-oxygen defects in p-type Czochralski silicon, 2017.
  - 76. Morishige AE, Jensen MA, Needleman DB, et al. Lifetime spectroscopy investigation of light-induced degradation in p-type multicrystalline silicon PERC. *IEEE J Photovolt.* 2016;6:1466-1472. <https://doi.org/10.1109/JPHOTOV.2016.2606699>
  - 77. Jensen MA, Zhu Y, Looney EE, et al. Assessing the defect responsible for LeTID: temperature- and injection-dependent lifetime spectroscopy, Proc. 44th IEEE Photovolt Spec Conf. 2017: 3290-3294.
  - 78. Sen C, Kim M, Chen D, et al. Assessing the impact of thermal profiles on the elimination of light- and elevated-temperature-induced degradation. *IEEE J Photovolt.* 2019;9:40-48. <https://doi.org/10.1109/JPHOTOV.2018.2874769>
  - 79. Winter M, Walter D, Bredemeier D, Schmidt J. Light-induced lifetime degradation effects at elevated temperature in Czochralski-grown silicon beyond boron-oxygen-related degradation. *Sol Energy Mater sol Cells.* 2019;201:110060. <https://doi.org/10.1016/j.solmat.2019.110060>
  - 80. Kim M, Chen D, Abbott M, Wenham S, Hallam B. Role of hydrogen: formation and passivation of meta-stable defects due to hydrogen in silicon, in: AIP Conf. Proc., 2018: p. 130010. <https://doi.org/10.1063/1.5049329>
  - 81. Kang D, Sio HC, Xinyu Z, Wang Q, Jin H, Macdonald D. Letid in p-type and n-type mono-like and float-zone silicon, and their dependence on SiN<sub>x</sub> film properties, in: 36th Eur. Photovolt. Sol. Energy Conf. Exhib., 2019: pp. 318-321. <https://doi.org/10.4229/EUPVSEC20192019-2CV.2.5>
  - 82. Schmidt J, Bredemeier D, Walter DC. On the defect physics behind light and elevated temperature-induced degradation (LeTID) of multicrystalline silicon solar cells. *IEEE J Photovolt.* 2019;9:1497-1503. <https://doi.org/10.1109/JPHOTOV.2019.2937223>
  - 83. Bredemeier D, Walter DC, Schmidt J. Possible candidates for impurities in mc-Si wafers responsible for light-induced lifetime degradation and regeneration. *Sol RRL.* 2018;2:1700159. <https://doi.org/10.1002/solr.201700159>
  - 84. Jensen MA, Wieghold S, Poindexter JR, et al. Solubility and diffusivity: important metrics in the search for the root cause of light- and elevated temperature-induced degradation. *IEEE J Photovolt.* 2018;8: 448-455. <https://doi.org/10.1109/JPHOTOV.2018.2791411>
  - 85. Eberle R, Kwapl W, Schindler F, Glunz SW, Schubert MC. Firing temperature profile impact on light induced degradation in multicrystalline silicon. *Energy Procedia.* 2017;124:712-717. <https://doi.org/10.1016/j.egypro.2017.09.082>
  - 86. Wagner M, Wolny F, Hentsche M, et al. Correlation of the LeTID amplitude to the aluminium bulk concentration and oxygen precipitation in PERC solar cells. *Sol Energy Mater sol Cells.* 2018;187:176-188. <https://doi.org/10.1016/j.solmat.2018.06.009>
  - 87. Luka T, Turek M, Großer S, Hagendorf C. Microstructural identification of Cu in solar cells sensitive to light-induced degradation. *Phys Status Solidi Rapid Res Lett.* 2017;11:1600426. <https://doi.org/10.1002/pssr.201600426>
  - 88. Yli-koski M, Serué M, Modanese C, Vahlman H, Savin H. Solar energy materials and solar cells low-temperature dark anneal as pre-treatment for LeTID in multicrystalline silicon. *Sol Energy Mater sol Cells.* 2019;192:134-139. <https://doi.org/10.1016/j.solmat.2018.12.021>
  - 89. Savin H, Yli-Koski M, Haarhiltunen A. Role of copper in light induced minority-carrier lifetime degradation of silicon. *Appl Phys Lett.* 2009;95:152111. <https://doi.org/10.1063/1.3250161>
  - 90. Sachdeva R, Istratov AA, Weber ER. Recombination activity of copper in silicon. *Appl Phys Lett.* 2001;79:2937-2939. <https://doi.org/10.1063/1.1415350>
  - 91. Vahlman H, Haarhiltunen A, Kwapl W, Schön J, Inglese A, Savin H. Modeling of light-induced degradation due to Cu precipitation in p-type silicon. II. Comparison of simulations and experiments. *J Appl Phys.* 2017;121:195704. <https://doi.org/10.1063/1.4983455>
  - 92. Vargas C. Effects of dark and illuminated anneals on multicrystalline silicon wafers and on monocrystalline silicon wafers with carrier-selective contacts, PhD Thesis Dissertation - UNSW Sydney, 2019.
  - 93. Zuschlag A, Skorka D, Hahn G. Degradation and regeneration analysis in mc-Si, Conf Rec IEEE Photovolt Spec Conf. 2016:1051-1054. <https://doi.org/10.1109/PVSC.2016.7749772>
  - 94. Skorka D, Zuschlag A, Hahn G. Firing and gettering dependence of effective defect density in material exhibiting LeTID, in: AIP Conf. Proc., 2018: p. 130015. <https://doi.org/10.1063/1.5049334>
  - 95. Chakraborty S, Huang Y, Wilson M, Aberle AG, Li JB. Mitigating light and elevated temperature induced degradation in multicrystalline silicon wafers and PERC solar cells using phosphorus diffusion gettering. *Phys Status Solidi.* 2018;215:1800160. <https://doi.org/10.1002/pssa.201800160>
  - 96. Sperber D, Herguth A, Hahn G. Investigating possible causes of light induced degradation in boron-doped float-zone silicon, Proc 33rd EUPVSEC. 2017:565-568.
  - 97. Khan MU, Chen D, Jafari S, et al. Degradation and regeneration of radiation-induced defects in silicon: a study of vacancy-hydrogen interactions. *Sol Energy Mater Sol Cells.* 2019;200:109990. <https://doi.org/10.1016/j.solmat.2019.109990>
  - 98. Jensen MA, Zuschlag A, Wieghold S, et al. Evaluating root cause: the distinct roles of hydrogen and firing in activating light- and elevated

- temperature-induced degradation. *J Appl Phys.* 2018;124:085701. <https://doi.org/10.1063/1.5041756>
99. Bourret-Sicotte G, Hamer PG, Tweddle D, Bonilla RS, Wilshaw PR. Hydrogen related defects in float zone silicon investigated using a shielded hydrogen plasma, 2018 IEEE 7th World Conf. Photovolt. Energy Conversion, WCPEC 2018 - A Jt. Conf. 45th IEEE PVSC, 28th PVSEC 34th EU PVSEC. 2018:298–302. <https://doi.org/10.1109/PVSC.2018.8547713>
100. Chen D, Kim M, Shi J, et al. Defect engineering of p-type silicon heterojunction solar cells fabricated using commercial-grade low-lifetime silicon wafers. *Prog Photovolt Res Appl.* 2019; pip.3230. <https://doi.org/10.1002/pip.3230>
101. Lucovsky G, Tsu DV. Plasma enhanced chemical vapor deposition: differences between direct and remote plasma excitation. *J Vac Sci Technol a Vacuum, Surfaces, Film.* 1987;5:2231–2238. <https://doi.org/10.1116/1.574963>
102. Hamer P, Bourret-Sicotte G, Martins G, Wenham A, Bonilla RS, Wilshaw P. A novel source of atomic hydrogen for passivation of defects in silicon. *Phys Status Solidi Rapid Res Lett.* 2017;11: 1600448. <https://doi.org/10.1002/pssr.201600448>
103. Myers SM, Baskes MI, Birnbaum HK, et al. Hydrogen interactions with defects in crystalline solids. *Rev Mod Phys.* 1992;64:559–617. <https://doi.org/10.1103/RevModPhys.64.559>
104. Seager CH, Anderson RA. Electronic control of hydrogen debonding from phosphorus in silicon—is there an acceptor state of interstitial hydrogen? *Solid State Commun.* 1990;76:285–288. [https://doi.org/10.1016/0038-1098\(90\)90838-3](https://doi.org/10.1016/0038-1098(90)90838-3)
105. Herring C, Johnson NM, Van de Walle CG. Energy levels of isolated interstitial hydrogen in silicon. *Phys Rev B.* 2001;64:125209. <https://doi.org/10.1103/PhysRevB.64.125209>
106. Chevallier J, Aucouturier M. Hydrogen in crystalline semiconductors. *Semicond Sci Technol.* 1991;6:73–84. <https://doi.org/10.1088/0268-1242/6/2/001>
107. Walter DC, Bredemeier D, Falster R, Voronkov VV, Schmidt J. Easy-to-apply methodology to measure the hydrogen concentration in boron-doped crystalline silicon. *Sol Energy Mater sol Cells.* 2019;200: 109970. <https://doi.org/10.1016/j.solmat.2019.109970>
108. Bredemeier D, Walter DC, Schmidt J. Lifetime degradation in multicrystalline silicon under illumination at elevated temperature: indications for the involvement of hydrogen, in: AIP Conf. Proc., 2018: p. 130001. <https://doi.org/10.1063/1.5049320>
109. Bredemeier D, Walter DC, Heller R, Schmidt J. Impact of hydrogen-rich silicon nitride material properties on light-induced lifetime degradation in multicrystalline silicon. *Phys Status Solidi Rapid Res Lett.* 2019;13:1900201. <https://doi.org/10.1002/pssr.201900201>
110. Winter C, Zuschlag A, Skorka D, Hahn G. Influence of dielectric layers and thermal load on LeTID. *AIP Conf Proc.* 2018;1999:2–6. <https://doi.org/10.1063/1.5049339>
111. Varshney U, Abbott M, Ciesla A, et al. Evaluating the impact of SiN<sub>x</sub> thickness on lifetime degradation in silicon. *IEEE J Photovolt.* 2019;9: 601–607. <https://doi.org/10.1109/JPHOTOV.2019.2896671>
112. Fung TH, Kim M, Chen D, et al. Influence of bound hydrogen states on carrier-induced degradation in multi-crystalline silicon, in: AIP Conf. Proc., 2018: p. 130004. <https://doi.org/10.1063/1.5049323>
113. McQuaid SA, Binns MJ, Newman RC, Lightowers EC, Clegg JB. Solubility of hydrogen in silicon at 1300°C. *Appl Phys Lett.* 1993;62: 1612–1614. <https://doi.org/10.1063/1.108602>
114. Voronkov VV, Falster R. Formation, dissociation, and diffusion of various hydrogen dimers in silicon. *Phys Status Solidi.* 2017;254: 1600779. <https://doi.org/10.1002/pssb.201600779>
115. Van de Walle CG, Neugebauer J. Hydrogen in semiconductors. *Annu Rev Mat Res.* 2006;36:179–198. <https://doi.org/10.1146/annurev.matsci.36.010705.155428>
116. Wenham S, Cisela A, Bagnall D, et al. Advanced hydrogen passivation that mitigates hydrogen-induced recombination (hir) and surface passivation deterioration in pv devices, US20190371959A1, 2019.
117. Nickel NH, Anderson GB, Johnson NM, Walker J. Nucleation of hydrogen-induced platelets in silicon. *Phys Rev B - Condens Matter Mater Phys.* 2000;62:8012–8015. <https://doi.org/10.1103/PhysRevB.62.8012>
118. Wang PA. Industrial challenges for thin wafer manufacturing, in: Conf. Rec. 2006 IEEE 4th World Conf. Photovolt. Energy Conversion, WCPEC-4, IEEE, 2006: pp. 1179–1182. <https://doi.org/10.1109/WCPEC.2006.279391>
119. Vargas C, Kim K, Coletti G, et al. Influence of silicon nitride and its hydrogen content of carrier-induced degradation in multicrystalline silicon, Proceeding 33rd Eur. Photovolt Sol Energy Conf Exhib Amsterdam. 2017:561.
120. Kang MH, Ryu K, Upadhyaya A, Rohatgi A. Optimization of SiN AR coating for Si solar cells and modules through quantitative assessment of optical and efficiency loss mechanism. *Prog Photovolt Res Appl.* 2011;19:983–990. <https://doi.org/10.1002/pip.1095>
121. Wang Z, Shen H, Hu D, et al. Influence of double current injection annealing on anti-LID effect in mono-like cast silicon PERC solar cells. *J Mater Sci Mater Electron.* 2020;31(4):3221–3227. <https://doi.org/10.1007/s10854-020-02870-5>
122. Hamer P, Chan C, Bonilla RS, et al. Hydrogen induced contact resistance in PERC solar cells. *Sol Energy Mater sol Cells.* 2018;184:91–97. <https://doi.org/10.1016/j.solmat.2018.04.036>
123. Hallam B, Herguth A, Hamer P, et al. Eliminating light-induced degradation in commercial p-type Czochralski silicon solar cells. *Appl Sci.* 2017;8:10. <https://doi.org/10.3390/app8010010>
124. Hallam BJ, Hamer PG, Wang S, et al. Advanced hydrogenation of dislocation clusters and boron-oxygen defects in silicon solar cells. *Energy Procedia.* 2015;77:799–809. <https://doi.org/10.1016/j.egypro.2015.07.113>
125. Hamer P, Hallam B, Abbott M, Wenham S. Accelerated formation of the boron-oxygen complex in p-type Czochralski silicon. *Phys Status Solidi Rapid Res Lett.* 2015;9:297–300. <https://doi.org/10.1002/pssr.201510064>
126. Peral A, Dastgheib-Shirazi A, Fano V, Jimeno JC, Hahn G, del Canizo C. Impact of extended contact cofiring on multicrystalline silicon solar cell parameters. *IEEE J Photovolt.* 2017;7:91–96. <https://doi.org/10.1109/JPHOTOV.2016.2621342>
127. Sen C, Chan C, Hamer P, et al. Annealing prior to contact firing: a potential new approach to suppress LeTID. *Sol Energy Mater sol Cells.* 2019;200:109938. <https://doi.org/10.1016/j.solmat.2019.109938>
128. Skorka D, Zuschlag A, Hahn G. Spatially resolved degradation and regeneration kinetics in mc-Si. Proc. 32nd Eur. Photovolt. Sol. Energy Conf. Exhib. 2016:643–646. <https://doi.org/10.1017/CBO9781107415324.004>
129. Bredemeier D, Walter DC, Pernau T, Romer O, Schmidt J. Production compatible remedy against LETID in high-performance multicrystalline silicon solar cells, 35th Eur. Photovolt. Sol. Energy Conf. Exhib. 2018:406–409. <https://doi.org/10.4229/35thEUPVSEC20182018-2CO.9.4>
130. Sharma R, Chong AP, Li JB, Aberle AG, Huang Y. Role of post-metallization anneal sequence and forming gas anneal to mitigate light and elevated temperature induced degradation of multicrystalline silicon solar cells. *Sol Energy Mater sol Cells.* 2019;195: 160–167. <https://doi.org/10.1016/j.solmat.2019.02.036>
131. Yli-Koski M, Pasanen TP, Heikkilä I, Serué M, Savin H. Low-T anneal as cure for letid in mc-Si PERC cells, in: AIP Conf. Proc., 2019: p. 140013. <https://doi.org/10.1063/1.5123900>

132. Varshney U, Chan C, Hoex B, et al. Controlling light- and elevated-temperature-induced degradation with thin film barrier layers. *IEEE J Photovolt.* 2020;10:19–27. <https://doi.org/10.1109/JPHOTOV.2019.2945199>
133. Yao Z, Zhang D, Wu J, Jiang F, Xing G, Su X. Evolution of LeTID defects in industrial multi-crystalline silicon wafers under laser illumination—dependency of wafer position in brick and temperature. *Sol Energy Mater sol Cells.* 2020;218:110735. <https://doi.org/10.1016/j.solmat.2020.110735>
134. Hamer P, Hallam B, Bonilla RS, Altermatt PP, Wilshaw P, Wenham S. Modelling of hydrogen transport in silicon solar cell structures under equilibrium conditions. *J Appl Phys.* 2018;123:043108. <https://doi.org/10.1063/1.5016854>
135. Wilking S, Ebert S, Herguth A, Hahn G. Influence of hydrogen effusion from hydrogenated silicon nitride layers on the regeneration of boron-oxygen related defects in crystalline silicon. *J Appl Phys.* 2013;114:194512. <https://doi.org/10.1063/1.4833243>
136. Varshney U, Abbott M, Ciesla A, et al. Controlling light- and elevated-temperature-induced degradation by thin film barrier layers, 9th Int. Conf. Cryst. Silicon Photovoltaics. 2019.

**How to cite this article:** Chen D, Vaqueiro Contreras M, Ciesla A, et al. Progress in the understanding of light- and elevated temperature-induced degradation in silicon solar cells: A review. *Prog Photovolt Res Appl.* 2021;29(11):1180–1201. <https://doi.org/10.1002/pip.3362>